

# Universality of the amplitude shift in fast two-pulse collisions in weakly perturbed linear physical systems

Quan M. Nguyen<sup>1</sup>, Toan T. Huynh<sup>2,3</sup>, and Avner Peleg<sup>4</sup>

<sup>1</sup>*Department of Mathematics, International University, Vietnam National University-HCMC, Ho Chi Minh City, Vietnam*

<sup>2</sup>*Department of Mathematics, University of Science, Vietnam National University-HCMC, Ho Chi Minh City, Vietnam*

<sup>3</sup>*Department of Mathematics, University of Medicine and Pharmacy at Ho Chi Minh City, Ho Chi Minh City, Vietnam and*

<sup>4</sup>*Department of Exact Sciences, Afeka College of Engineering, Tel Aviv 69988, Israel*

(Dated: January 9, 2022)

## Abstract

We demonstrate that the amplitude shifts in fast two-pulse collisions in perturbed linear physical systems with weak nonlinear dissipation exhibit universal soliton-like behavior. The behavior is demonstrated for linear optical waveguides with weak cubic loss and for systems described by linear diffusion-advection models with weak quadratic loss. We show that in both systems, the expressions for the collision-induced amplitude shifts due to the nonlinear loss have the same form as the expression obtained for a fast collision between two solitons of the nonlinear Schrödinger equation in the presence of weak cubic loss. Furthermore, we show that the expressions for the amplitude shifts are universal in the sense that they are independent of the exact details of the initial pulse shapes. We demonstrate the universal soliton-like behavior of the collision-induced amplitude shifts by carrying out numerical simulations with the two perturbed coupled linear evolution models with three different initial conditions corresponding to pulses with exponentially decreasing tails, pulses with power-law decreasing tails, and pulses that are initially nonsmooth and that develop significant tails during the collision. In all six cases we observe very good agreement between the analytic predictions for the amplitude shifts and the results of the numerical simulations.

## I. INTRODUCTION

The stable shape preserving pulse solutions of nonlinear wave models, which are known as solitons, appear in a variety of fields, including optics [1, 2], condensed matter physics [3], hydrodynamics [4, 5], and plasma physics [6]. One of the main properties characterizing solitons is their robustness in soliton collisions, that is, the fact that the solitons do not change their shape in the collisions. Another important property of solitons, which is manifested in fast inter-soliton collisions, is the simple form of the scaling relations for collision-induced changes of soliton parameters, such as position, phase, amplitude, and frequency [7]. This property holds both in the absence of perturbations and in the presence of weak perturbations to the integrable nonlinear wave model. Consider for example fast collisions between two solitons of the cubic nonlinear Schrödinger (NLS) equation, which is one of the most widely used nonlinear wave models in physics [3–5]. In the absence of perturbations, the collision-induced changes in the phase and position of soliton 1, for example, scale as  $\eta_2/|\Delta\beta|$  and  $-\eta_2/\Delta\beta^2$ , where  $\eta_j$  with  $j = 1, 2$  are the soliton amplitudes,  $\Delta\beta = \beta_2 - \beta_1$ , and  $\beta_j$  with  $j = 1, 2$  are the soliton frequencies [4, 8, 9]. Furthermore, during fast collisions between NLS solitons in the presence of a weak perturbation due to cubic loss, the solitons experience amplitude and frequency shifts, which scale as  $-\epsilon_3\eta_1\eta_2/|\Delta\beta|$  and  $-\epsilon_3\eta_1^2\eta_2/\Delta\beta^2$  for soliton 1, where  $\epsilon_3$  is the cubic loss coefficient [10]. Similar simple scaling relations hold for fast two-pulse collisions of NLS solitons in the presence of other weak perturbations, such as delayed Raman response [9, 11–15], and higher-order nonlinear loss [16].

The simple form of the scaling relations for collision-induced changes of soliton parameters can be attributed to the shape preserving and stability properties of the solitons [9, 10, 16]. The latter two properties are related with the integrability of the nonlinear wave model. Therefore, one might also relate the simple form of the scaling relations for changes in soliton parameters in fast two-soliton collisions to the integrability of the model. One might expect a very different behavior for collisions between pulses that are not shape preserving, since in this case, it is expected that changes in pulse shape or instability would lead to the breakdown of the simple dynamics observed in fast two-soliton collisions. This expectation is especially typical for linear physical systems that are weakly perturbed by nonlinear dissipation, since the pulses of the linear systems are in general not shape preserving [1, 17, 18]. However, in Ref. [19], we showed that the opposite might in fact be true. That is, we

demonstrated that the amplitude shifts in fast two-pulse collisions in linear physical systems, weakly perturbed by nonlinear dissipation, exhibit soliton-like scaling behavior. The behavior was demonstrated for collisions between Gaussian pulses of the following central physical systems: (1) linear optical waveguides with weak cubic loss; (2) systems described by linear diffusion-advection models with weak quadratic loss. We showed that in both cases, the expressions for the amplitude shifts in fast collisions between two Gaussian pulses have the same form as the expression for the amplitude shift in a fast collision between two solitons of the cubic NLS equation in the presence of weak cubic loss. The analytic predictions were confirmed by numerical simulations with the corresponding perturbed coupled linear evolution models.

The study in Ref. [19] was limited to fast collisions between Gaussian pulses. Therefore, based on the results of Ref. [19], it is unclear if the soliton-like behavior of the collision-induced amplitude shift is universal in the sense that it does not depend on the details of the initial pulse shapes. In the current paper we address this important question. More specifically, we show that the simple soliton-like form of the expressions for the collision-induced amplitude shifts is universal in the sense that it is independent of the exact details of the initial pulse shapes. This is done for both linear optical waveguides with weak cubic loss and for systems described by linear diffusion-advection models with weak quadratic loss. We explain the universal soliton-like form of the expressions for the collision-induced amplitude shifts by noting that changes in pulse shapes occurring during a collision due to the effects of dispersion or diffusion can be neglected for fast collisions, and by noting the conservation of the total energies (or total masses) of the pulses by the unperturbed linear evolution models. Furthermore, we demonstrate the universal behavior of the amplitude shifts by carrying out numerical simulations with the two perturbed coupled linear evolution models with three different initial conditions corresponding to pulses with exponentially decreasing tails, pulses with power-law decreasing tails, and pulses that are initially nonsmooth. We find very good agreement between the analytic predictions for the amplitude shifts and the results of the numerical simulations in all six cases. Surprisingly, the analytic predictions hold even for collisions between pulses with initially nonsmooth shapes in linear optical waveguides despite of the fast generation of significant pulse tails in this case. We explain the good agreement between the analytic and numerical results in the latter case by noting that during fast collisions most of the pulse energies are still contained in the main bodies

of the pulses, and by noting the conservation of the total energies of the two pulses by the unperturbed linear propagation model.

The rest of the paper is organized as follows. In Sec. II, we obtain the expression for the collision-induced amplitude shift in a fast two-pulse collision in a linear optical waveguide with weak linear and cubic loss. We show that this expression is universal in the sense that it is independent of the details of the initial pulse shapes. We then present a comparison of the analytic expression with results of numerical simulations with the perturbed coupled linear propagation model for three major types of pulses. In Sec. III, we obtain the expression for the amplitude shift in a fast collision between two concentration pulses in systems described by perturbed coupled linear diffusion-advection models with weak linear and quadratic loss. We then show that this expression is universal. Furthermore, we compare the analytic expression for the amplitude shift with results of numerical simulations with the perturbed coupled linear diffusion-advection model for three main types of pulses. Section IV is devoted to our conclusions. In Appendix A, we derive the relations between the collision-induced amplitude shifts and the collision-induced changes in pulse shapes. A description of the procedures used for calculating the values of the collision-induced amplitude shift from the analytic expressions and from results of numerical simulations is provided in Appendix B.

## II. FAST COLLISIONS IN LINEAR OPTICAL WAVEGUIDES

### A. Propagation model and initial pulse shapes

We consider the dynamics of fast collisions between two pulses of light in linear optical waveguides with weak linear and cubic loss. The dynamics of the collision can be described by the following system of perturbed coupled linear propagation equations [10, 19, 20]:

$$\begin{aligned}
 i\partial_z\psi_1 - \text{sgn}(\tilde{\beta}_2)\partial_t^2\psi_1 &= -i\epsilon_1\psi_1 - i\epsilon_3|\psi_1|^2\psi_1 - 2i\epsilon_3|\psi_2|^2\psi_1, \\
 i\partial_z\psi_2 + id_1\partial_t\psi_2 - \text{sgn}(\tilde{\beta}_2)\partial_t^2\psi_2 &= -i\epsilon_1\psi_2 - i\epsilon_3|\psi_2|^2\psi_2 \\
 &\quad - 2i\epsilon_3|\psi_1|^2\psi_2,
 \end{aligned} \tag{1}$$

where  $\psi_1$  and  $\psi_2$  are the envelopes of the electric fields of the pulses,  $z$  is propagation distance, and  $t$  is time [21]. In Eq. (1),  $d_1$  is the group velocity coefficient,  $\tilde{\beta}_2$  is the second-order dispersion coefficient, and  $\epsilon_1$  and  $\epsilon_3$  are the linear and cubic loss coefficients, which

satisfy  $0 < \epsilon_1 \ll 1$  and  $0 < \epsilon_3 \ll 1$ . The terms  $-\text{sgn}(\tilde{\beta}_2)\partial_t^2\psi_j$  on the left hand side of Eq. (1) are due to the effects of second-order dispersion, while  $id_1\partial_t\psi_2$  is associated with the group velocity difference. The first terms on the right hand side of Eq. (1) describe linear loss effects, while the second and third terms describe intra-pulse and inter-pulse effects due to cubic loss. Note that the perturbed coupled propagation model (1) is based on the assumption that the effects of cubic (Kerr) nonlinearity can be neglected. This assumption was successfully used in previous experimental and theoretical works, see e.g., Refs. [22–25]. In addition, it is assumed that the nonlinear loss is weak, and as a result, the effects of higher-order loss are also neglected. We emphasize, however, that the effects of higher-order loss on the collision-induced amplitude shift can be calculated in a manner similar to the one described in Sec. II B (see also, Ref. [26], where the calculation was carried out for collisions between Gaussian pulses).

We are interested in demonstrating universal behavior of the amplitude shift in fast two-pulse collisions in the sense that the amplitude shift is not very sensitive to the exact details of the pulse shape. We therefore consider fast collisions between pulses with generic initial pulse shapes and with tails that decay sufficiently fast, such that the values of the integrals  $\int_{-\infty}^{\infty} dt |\psi_j(t, 0)|^2$  are finite. We assume that the pulses can be characterized by initial amplitudes  $A_j(0)$ , initial widths  $W_{j0}$ , initial positions  $y_{j0}$ , and initial phases  $\alpha_{j0}$ . To illustrate the universal behavior of the collision-induced amplitude shift we consider three prototypical initial pulse shapes, which represent three major types of behavior of the pulse tails before and during the collisions. More specifically, we consider the following three types of pulses: (1) pulses with exponentially decreasing tails, (2) pulses with power-law decreasing tails, (3) pulses that are initially nonsmooth and that develop significant tails during the propagation. For concreteness, we demonstrate the universal behavior of the amplitude shift using the following representative initial pulses: hyperbolic secant pulses in (1), generalized Cauchy-Lorentz pulses in (2), and square pulses in (3). The initial envelopes of the electric fields for these pulses are given by

$$\psi_j(t, 0) = A_j(0) \text{sech}[(t - y_{j0})/W_{j0}] \exp(i\alpha_{j0}), \quad (2)$$

with  $j = 1, 2$  for hyperbolic secant pulses, by

$$\psi_j(t, 0) = \frac{A_j(0) \exp(i\alpha_{j0})}{1 + 2[(t - y_{j0})/W_{j0}]^4}, \quad (3)$$

with  $j = 1, 2$  for generalized Cauchy-Lorentz pulses, and by

$$\psi_j(t, 0) = \begin{cases} A_j(0) \exp(i\alpha_{j0}) & \text{for } |t - y_{j0}| \leq W_{j0}/2, \\ 0 & \text{for } |t - y_{j0}| > W_{j0}/2, \end{cases} \quad (4)$$

with  $j = 1, 2$  for square pulses. We emphasize, however, that similar behavior of the collision-induced amplitude shift is observed for other choices of the initial pulse shapes.

## B. Calculation of the collision-induced amplitude shift

The expressions for the collision-induced amplitude shifts are obtained under the assumption of a complete fast two-pulse collision. The complete collision assumption means that the two pulses are well separated at  $z = 0$  and at the final propagation distance  $z = z_f$ . To explain the implications of the fast collision assumption, we define the collision length  $\Delta z_c$ , which is the distance along which the envelopes of the colliding pulses overlap, by  $\Delta z_c = W_0/|d_1|$ , where for simplicity we assume  $W_{10} = W_{20} = W_0$ . The fast collision assumption then means that  $\Delta z_c$  is the shortest length scale in the problem. In particular,  $\Delta z_c \ll z_D$ , where  $z_D = W_0^2/2$  is the length scale characterizing the effects of second-order dispersion on single-pulse propagation (the dispersion length). Using the definitions of  $\Delta z_c$  and  $z_D$ , we obtain  $W_0|d_1|/2 \gg 1$ , as the condition for a fast two-pulse collision.

We now show that the condition  $W_0|d_1|/2 \gg 1$  is clearly satisfied for collisions in massive multichannel weakly perturbed linear optical waveguide systems with tens or hundreds of frequency channels. Consider as an example a multichannel linear optical fiber system with a total wavelength difference  $\Delta\lambda = \lambda_2 - \lambda_1 = 0.045 \mu\text{m}$ , where  $\lambda_1 = 1.549 \mu\text{m}$  is the wavelength for the highest frequency channel and  $\lambda_2 = 1.594 \mu\text{m}$  is the wavelength for the lowest frequency channel. These values are identical to the ones used in the multichannel optical fiber transmission experiment with 109 channels reported in Ref. [27]. The group refractive index values for these wavelengths are  $n_{g1} = 1.4626$  and  $n_{g2} = 1.4629$ , respectively [1, 28, 29]. Assuming in addition that the pulse width is 20 ps and that  $|\tilde{\beta}_2| = 1 \text{ ps}^2/\text{km}$ , which are typical values for multichannel transmission at 10 Gb/s per channel, we obtain  $W_0|d_1|/2 = 2 \times 10^4 \gg 1$  for collisions between pulses from the two outermost frequency channels. Moreover, since the frequency difference between adjacent channels in multichannel transmission is constant, we obtain that in a system with 109 channels  $W_0|d_1|/2 \simeq 185.2 \gg 1$  for collisions between pulses from adjacent channels. Therefore, the condition for a fast

collision is satisfied for all collisions in this linear optical fiber transmission system. As a second example, consider linear multichannel transmission in a silicon waveguide with  $\Delta\lambda = \lambda_2 - \lambda_1 = 0.05 \mu\text{m}$ ,  $\lambda_1 = 0.75 \mu\text{m}$ , and  $\lambda_2 = 0.8 \mu\text{m}$ . The group refractive index values for these wavelengths are  $n_{g1} = 4.3597$  and  $n_{g2} = 4.3285$ , respectively [30]. Assuming that the pulse width is 20 ps and that  $|\tilde{\beta}_2| = 1 \text{ ps}^2/\text{km}$ , we find  $W_0|d_1|/2 = 2.08 \times 10^6 \gg 1$  for collisions between pulses from the two outermost frequency channels. Furthermore, we obtain that in a multichannel system with 109 channels  $W_0|d_1|/2 \simeq 1.926 \times 10^4 \gg 1$  for collisions between pulses from adjacent frequency channels. Thus, the condition for a fast collision is satisfied for all collisions in this linear silicon waveguide transmission system.

The perturbation technique for calculating the collision-induced amplitude shift was first presented in our work in Ref. [19]. We present here a review of this perturbation technique along with some important features that were not discussed in Ref. [19]. Our perturbation procedure is a generalization of the perturbative technique, developed in Refs. [31, 32] for calculating the effects of weak perturbations on fast two-soliton collisions. Following the perturbative calculation for the two-soliton collision, we look for a solution of Eq. (1) in the form

$$\psi_j(t, z) = \psi_{j0}(t, z) + \phi_j(t, z), \quad (5)$$

where  $j = 1, 2$ ,  $\psi_{j0}$  are the solutions of Eq. (1) without the inter-pulse interaction terms, and  $\phi_j$  describe corrections to  $\psi_{j0}$  due to inter-pulse interaction. By definition,  $\psi_{10}$  and  $\psi_{20}$  satisfy the following two weakly perturbed linear propagation equations

$$i\partial_z\psi_{10} - \text{sgn}(\tilde{\beta}_2)\partial_t^2\psi_{10} = -i\epsilon_1\psi_{10} - i\epsilon_3|\psi_{10}|^2\psi_{10}, \quad (6)$$

and

$$\begin{aligned} i\partial_z\psi_{20} + id_1\partial_t\psi_{20} - \text{sgn}(\tilde{\beta}_2)\partial_t^2\psi_{20} = \\ -i\epsilon_1\psi_{20} - i\epsilon_3|\psi_{20}|^2\psi_{20}. \end{aligned} \quad (7)$$

We now substitute the ansatz (5) into Eq. (1) and use Eqs. (6) and (7) to obtain equations for the  $\phi_j$ . We focus attention on the calculation of  $\phi_1$ , as the calculation of  $\phi_2$  is similar. Taking into account only leading-order effects of the collision, i.e., effects of order  $\epsilon_3$ , we can neglect terms containing  $\phi_j$  on the right hand side of the resulting equation. We therefore obtain:

$$i\partial_z\phi_1 - \text{sgn}(\tilde{\beta}_2)\partial_t^2\phi_1 = -2i\epsilon_3|\psi_{20}|^2\psi_{10}. \quad (8)$$

We continue to follow the perturbation procedure for fast two-soliton collisions and substitute  $\psi_{j0}(t, z) = \Psi_{j0}(t, z) \exp[i\chi_{j0}(t, z)]$  and  $\phi_1(t, z) = \Phi_1(t, z) \exp[i\chi_{10}(t, z)]$  into Eq. (8), where  $\Psi_{j0}$  and  $\chi_{j0}$  are real-valued. We arrive at the following equation for  $\Phi_1$ :

$$\begin{aligned} i\partial_z\Phi_1 - (\partial_z\chi_{10})\Phi_1 - \text{sgn}(\tilde{\beta}_2) [\partial_t^2\Phi_1 + 2i(\partial_t\chi_{10})\partial_t\Phi_1 \\ + i(\partial_t^2\chi_{10})\Phi_1 - (\partial_t\chi_{10})^2\Phi_1] = -2i\epsilon_3\Psi_{20}^2\Psi_{10}. \end{aligned} \quad (9)$$

The term on the right hand side of Eq. (9) is of order  $\epsilon_3$ . In addition, since the collision length  $\Delta z_c$  is of order  $1/|d_1|$ , the term  $i\partial_z\Phi_1$  is of order  $|d_1| \times O(\Phi_1)$ . Equating the orders of  $i\partial_z\Phi_1$  and  $-2\epsilon_3\Psi_{20}^2\Psi_{10}$ , we find that  $\Phi_1$  is of order  $\epsilon_3/|d_1|$ . In addition, we observe that all other terms on the left hand side of Eq. (9) are of order  $\epsilon_3/|d_1|$  or higher, and can therefore be neglected. As a result, the equation for  $\Phi_1$  in the leading order of the perturbative calculation is:

$$\partial_z\Phi_1 = -2\epsilon_3\Psi_{20}^2\Psi_{10}. \quad (10)$$

Equation (10) has the same form as the equation obtained for a fast collision between two solitons of the NLS equation in the presence of weak cubic loss (see Eq. (9) in Ref. [10]). We also note that since the  $\Psi_{j0}$  are real-valued,  $\Phi_1$  is real-valued as well.

We calculate the net collision-induced amplitude shift of pulse 1 from the net collision-induced change in  $\Phi_1$ . For this purpose, we denote by  $z_c$  the collision distance, which is the distance at which the maxima of  $|\psi_j(t, z)|$  coincide. In a fast collision, the collision takes place in a small interval  $[z_c - \Delta z_c, z_c + \Delta z_c]$  around  $z_c$ . Therefore, the net collision-induced change in the envelope of pulse 1  $\Delta\Phi_1(t, z_c)$  can be evaluated by:  $\Delta\Phi_1(t, z_c) = \Phi_1(t, z_c + \Delta z_c) - \Phi_1(t, z_c - \Delta z_c)$ . To calculate  $\Delta\Phi_1(t, z_c)$ , we introduce the approximation  $\Psi_{j0}(t, z) = A_j(z)\tilde{\Psi}_{j0}(t, z)$ , where  $\tilde{\psi}_{j0}(t, z) = \tilde{\Psi}_{j0}(t, z) \exp[i\chi_{j0}(t, z)]$  is the solution of the unperturbed linear propagation equation with unit amplitude. We then substitute the approximate expressions for  $\Psi_{j0}$  into Eq. (10) and integrate with respect to  $z$  over the interval  $[z_c - \Delta z_c, z_c + \Delta z_c]$ . This calculation yields:

$$\Delta\Phi_1(t, z_c) = -2\epsilon_3 \int_{z_c - \Delta z_c}^{z_c + \Delta z_c} dz' A_1(z') A_2^2(z') \tilde{\Psi}_{10}(t, z') \tilde{\Psi}_{20}^2(t, z'). \quad (11)$$

The only function on the right hand side of Eq. (11) that contains fast variations in  $z$ , which are of order 1, is  $\tilde{\Psi}_{20}$ . We can therefore approximate  $A_1(z)$ ,  $A_2(z)$ , and  $\tilde{\Psi}_{10}(t, z)$  by  $A_1(z_c^-)$ ,



$A_2(z_c^-)$ , and  $\tilde{\Psi}_{10}(t, z_c)$ , where  $A_j(z_c^-)$  is the limit from the left of  $A_j$  at  $z_c$ . Furthermore, we can take into account only the fast dependence of  $\tilde{\Psi}_{20}$  on  $z$ , i.e., the  $z$  dependence that is contained in the factors  $y = t - y_{20} - d_1 z$ . Denoting this approximation of  $\tilde{\Psi}_{20}(t, z)$  by  $\bar{\Psi}_{20}(y, z_c)$ , we obtain:

$$\Delta\Phi_1(t, z_c) = -2\epsilon_3 A_1(z_c^-) A_2^2(z_c^-) \tilde{\Psi}_{10}(t, z_c) \times \int_{z_c - \Delta z_c}^{z_c + \Delta z_c} dz' \bar{\Psi}_{20}^2(t - y_{20} - d_1 z', z_c). \quad (12)$$

Since the integrand on the right hand side of Eq. (12) is sharply peaked at a small interval around  $z_c$ , we can extend the integral's limits to  $-\infty$  and  $\infty$ . We also change the integration variable from  $z'$  to  $y = t - y_{20} - d_1 z'$  and obtain:

$$\Delta\Phi_1(t, z_c) = -\frac{2\epsilon_3 A_1(z_c^-) A_2^2(z_c^-)}{|d_1|} \tilde{\Psi}_{10}(t, z_c) \int_{-\infty}^{\infty} dy \bar{\Psi}_{20}^2(y, z_c). \quad (13)$$

In Appendix A, we show that the net collision-induced amplitude shift of pulse 1  $\Delta A_1^{(c)}$  is related to the net collision-induced change in the envelope of the pulse  $\Delta\Phi_1(t, z_c)$  by:

$$\Delta A_1^{(c)} = \left[ \int_{-\infty}^{\infty} dt \tilde{\Psi}_{10}^2(t, z_c) \right]^{-1} \int_{-\infty}^{\infty} dt \tilde{\Psi}_{10}(t, z_c) \Delta\Phi_1(t, z_c). \quad (14)$$

Substitution of Eq. (13) into Eq. (14) yields the following expression for the net collision-induced amplitude shift of pulse 1:

$$\Delta A_1^{(c)} = -\frac{2\epsilon_3 A_1(z_c^-) A_2^2(z_c^-)}{|d_1|} \int_{-\infty}^{\infty} dy \bar{\Psi}_{20}^2(y, z_c). \quad (15)$$

Note that

$$\int_{-\infty}^{\infty} dy \bar{\Psi}_{20}^2(y, z_c) = \int_{-\infty}^{\infty} dt \tilde{\Psi}_{20}^2(t, z_c) = \int_{-\infty}^{\infty} dt |\tilde{\psi}_{20}(t, z_c)|^2.$$

But since  $\int_{-\infty}^{\infty} dt |\tilde{\psi}_{20}(t, z)|^2$  is a conserved quantity of the unperturbed linear propagation equation, the following relations hold

$$\int_{-\infty}^{\infty} dt |\tilde{\psi}_{20}(t, z_c)|^2 = \int_{-\infty}^{\infty} dt |\tilde{\psi}_{20}(t, 0)|^2 = \int_{-\infty}^{\infty} dt \tilde{\Psi}_{20}^2(t, 0) = \text{const.}$$

Thus, we can replace the integral on the right hand side of Eq. (15) by  $\int_{-\infty}^{\infty} dt \tilde{\Psi}_{20}^2(t, 0)$  and obtain

$$\Delta A_1^{(c)} = -\frac{2\epsilon_3 A_1(z_c^-) A_2^2(z_c^-)}{|d_1|} \int_{-\infty}^{\infty} dt \tilde{\Psi}_{20}^2(t, 0). \quad (16)$$

We note that the collision-induced amplitude shift  $\Delta A_1^{(c)}$  depends only on the values of  $A_1(z_c^-)$ ,  $A_2(z_c^-)$ ,  $|d_1|$ , and on the initial total energy of pulse 2,  $\int_{-\infty}^{\infty} dt \tilde{\Psi}_{20}^2(t, 0)$ . The amplitude shift does not depend on any other properties of the initial pulses. Thus, the expression for the amplitude shift is universal in the sense that it is independent of the exact details of the initial pulse shapes. Equation (16) is expected to hold for generic pulse shapes  $\Psi_{j0}(t, z)$  with tails that decay sufficiently fast, such that the approximations leading from Eq. (11) to Eq. (13) are valid. Our numerical simulations with the coupled propagation model (1), whose results are presented in Sec. II C, reveal that Eq. (16) is valid even for pulses with power-law decreasing tails, such as generalized Cauchy-Lorentz pulses, and for pulses that are initially nonsmooth and that develop significant tails during the propagation, such as square pulses.

We now use Eq. (16) to obtain expressions for the amplitude shifts in fast collisions between hyperbolic secant pulses, generalized Cauchy-Lorentz pulses, and square pulses, whose initial envelopes are given by Eqs. (2), (3), and (4), respectively. We find that in all three cases, the amplitude shift of pulse 1 has the form

$$\Delta A_1^{(c)} = -C_P \epsilon_3 W_{20} A_1(z_c^-) A_2^2(z_c^-) / |d_1|, \quad (17)$$

where  $W_{20}$  is the initial pulse width of pulse 2 and  $C_P$  is a constant, whose value depends on the total initial energy of pulse 2. Furthermore, we find that  $C_P = 4$  for a collision between hyperbolic secant pulses,  $C_P = 3\pi/2^{7/4}$  for a collision between generalized Cauchy-Lorentz pulses, and  $C_P = 2$  for a collision between square pulses. In Ref. [10], we showed that the amplitude shift in a fast collision between two solitons of the NLS equation in the presence of weak cubic loss is given by:  $\Delta \eta_1^{(c)} = -4\epsilon_3 \eta_1(z_c^-) \eta_2(z_c^-) / |\Delta\beta|$  (see Eq. (11) in Ref. [10]). Noting that the soliton width is  $W_j = 1/\eta_j$ , we can express the collision-induced amplitude shift of the soliton as:

$$\Delta \eta_1^{(c)} = -4\epsilon_3 W_2(z_c^-) \eta_1(z_c^-) \eta_2^2(z_c^-) / |\Delta\beta|. \quad (18)$$

Thus, the expression for the collision-induced amplitude shift of the soliton has exactly the same form as the expression in Eq. (17) for a collision between two pulses of the linear propagation equation. We also observe that  $C_P = 4$  in a two-soliton collision and in a collision between two hyperbolic secant pulses of the linear propagation equation.

### C. Numerical simulations for different pulse shapes

Since the prediction of section II B for universal behavior of the collision-induced amplitude shift in fast two-pulse collisions is based on several simplifying assumptions, it is important to check this prediction by numerical simulations with the full propagation model (1). Equation (1) is numerically integrated by employing the split-step method with periodic boundary conditions [1, 33]. For concreteness and without loss of generality, we present the results of the simulations with parameter values  $\epsilon_1 = 0.01$ ,  $\epsilon_3 = 0.01$ , and  $\text{sgn}(\tilde{\beta}_2) = 1$ . Since we are interested in fast collisions, the values of  $d_1$  are varied in the intervals  $-60 \leq d_1 \leq -2$  and  $2 \leq d_1 \leq 60$ . To demonstrate the universal behavior of the collision-induced amplitude shift, we carry out the simulations with the three representative initial pulse shapes given by Eqs. (2)-(4), which correspond to hyperbolic secant pulses, generalized Cauchy-Lorentz pulses, and square pulses. The values of the initial amplitudes, initial widths, initial phases, and initial position of pulse 1 are chosen as  $A_j(0) = 1$ ,  $W_{j0} = 4$ ,  $\alpha_{j0} = 0$ , and  $y_{10} = 0$ . The initial position of pulse 2  $y_{20}$  and the final propagation distance  $z_f$  are chosen, such that the two pulses are well separated at  $z = 0$  and at  $z = z_f$ . In particular, we choose  $y_{20} = \pm 25$  and  $z_f = 4$  for hyperbolic secant pulses,  $y_{20} = \pm 20$  and  $z_f = 3$  for generalized Cauchy-Lorentz pulses, and  $y_{20} = \pm 6$  and  $z_f = 4.5$  for square pulses. We emphasize, however, that results similar to the ones presented below are obtained in numerical simulations with other physical parameter values. For each of the three types of pulse shapes we present the dependence of  $\Delta A_1^{(c)}$  on  $d_1$  obtained in the simulations together with the analytic prediction of Eq. (17). We also discuss the behavior of the relative error in the approximation of  $\Delta A_1^{(c)}$ , which is defined by  $|\Delta A_1^{(c)(num)} - \Delta A_1^{(c)(th)}| \times 100 / |\Delta A_1^{(c)(th)}|$ . The procedures used for obtaining the values of  $\Delta A_1^{(c)}$  from Eq. (17) and for calculating  $\Delta A_1^{(c)}$  from the results of the numerical simulations are described in Appendix B.

We start by discussing the results of the numerical simulations for fast collisions between hyperbolic secant pulses. Figure 1 shows the initial pulse shapes  $|\psi_j(t, 0)|$ , and the pulse shapes  $|\psi_j(t, z)|$  obtained in the simulation with  $d_1 = 15$  at the intermediate distance  $z_i = 2 > z_c$ , and at the final distance  $z_f = 4$  [34]. Also shown is the analytic prediction for  $|\psi_j(t, z)|$ , which is obtained by employing Eq. (5). We observe very good agreement between the analytic prediction and the result of the numerical simulation at both  $z = z_i$  and  $z = z_f$ . In addition, we find that the pulses undergo broadening due to second-order dispersion and

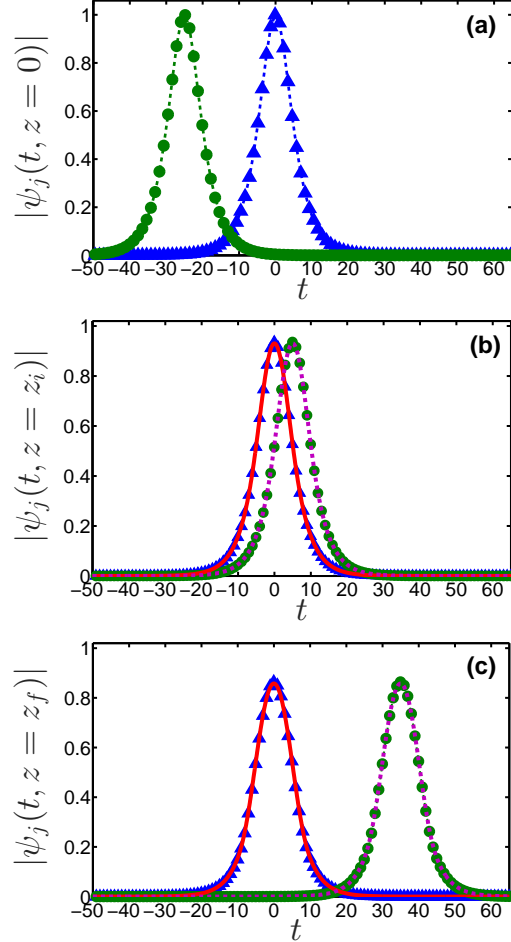


FIG. 1: (Color online) The pulse shapes  $|\psi_j(t, z)|$  at  $z = 0$  (a),  $z = z_i = 2$  (b), and  $z = z_f = 4$  (c) in a fast collision between two hyperbolic secant pulses in a linear waveguide with weak linear and cubic loss. The first-order dispersion coefficient is  $d_1 = 15$ . The blue triangles and green circles represent the initial pulse shapes  $|\psi_j(t, 0)|$  with  $j = 1, 2$  in (a), and the perturbation theory's prediction for  $|\psi_j(t, z)|$  with  $j = 1, 2$  in (b) and (c). The solid red and dashed magenta curves in (b) and (c) correspond to  $|\psi_j(t, z)|$  with  $j = 1, 2$ , obtained by numerical solution of Eq. (1).

that no significant tail develops up to the final distance  $z_f$ . The dependence of the collision-induced amplitude shift  $\Delta A_1^{(c)}$  on  $d_1$  obtained by the numerical simulations is shown in Fig. 2 along with the analytic prediction of Eq. (17). The agreement between the analytic prediction and the simulations results is very good. More specifically, the relative error in the approximation of  $\Delta A_1^{(c)}$  is less than 4.3% for  $10 \leq |d_1| \leq 60$  and less than 8.2% for  $2 \leq |d_1| < 10$ . Thus, the analytic prediction of Eq. (17) provides a good approximation for the actual value of the collision-induced amplitude shift even at  $d_1$  values that are not

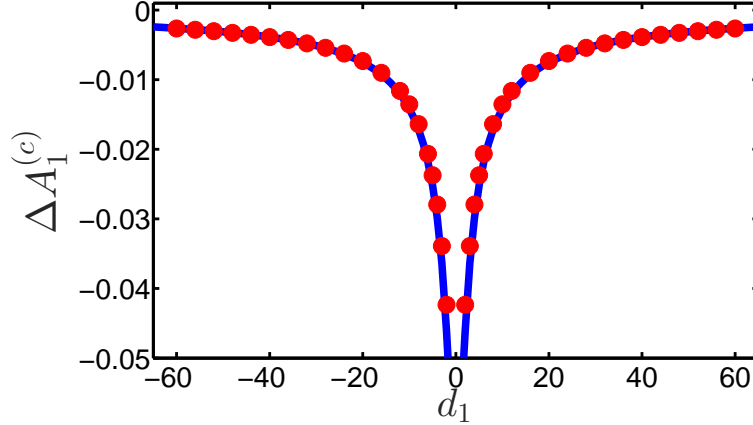


FIG. 2: (Color online) The collision-induced amplitude shift of pulse 1  $\Delta A_1^{(c)}$  vs the group velocity parameter  $d_1$  in a fast collision between two hyperbolic secant pulses in a linear waveguide with weak linear and cubic loss. The red circles correspond to the result obtained by numerical solution of Eq. (1). The solid blue curve represents the prediction of Eq. (17) with  $C_P = 4$ .

much larger than 1. These findings together with similar findings obtained in Ref. [19] for collisions between Gaussian pulses demonstrate the universal behavior of the amplitude shift in fast collisions between pulses with shapes that exhibit exponential or faster than exponential decrease with time.

Next, we consider fast collisions between generalized Cauchy-Lorentz pulses. The initial pulse shapes  $|\psi_j(t, 0)|$ , and the pulse shapes  $|\psi_j(t, z)|$  obtained in the simulation with  $d_1 = 15$  at  $z_i = 1.571 > z_c$  and at  $z_f = 3$  are shown in Fig. 3. The analytic prediction for  $|\psi_j(t, z)|$ , which is obtained with Eq. (5), is also shown. We observe that the pulses undergo considerable broadening and develop observable tails due to the effects of second-order dispersion. Despite of this, the agreement between the prediction of the perturbation theory and the simulation's result is very good at both  $z = z_i$  and  $z = z_f$ . The dependence of  $\Delta A_1^{(c)}$  on  $d_1$  obtained in the simulations is shown in Fig. 4 together with the analytic prediction of Eq. (17). We observe very good agreement between the results of the simulations and the analytic prediction. In particular, the relative error in the approximation of  $\Delta A_1^{(c)}$  is smaller than 2.9% for  $10 \leq |d_1| \leq 60$  and smaller than 6.8% for  $2 \leq |d_1| < 10$ . Similar results are obtained for other values of the physical parameters and for other pulse shapes with power-law decreasing tails. Thus, our current study extends the results of Ref. [19], in which it was assumed that the initial pulse shapes must possess tails that exhibit exponential or

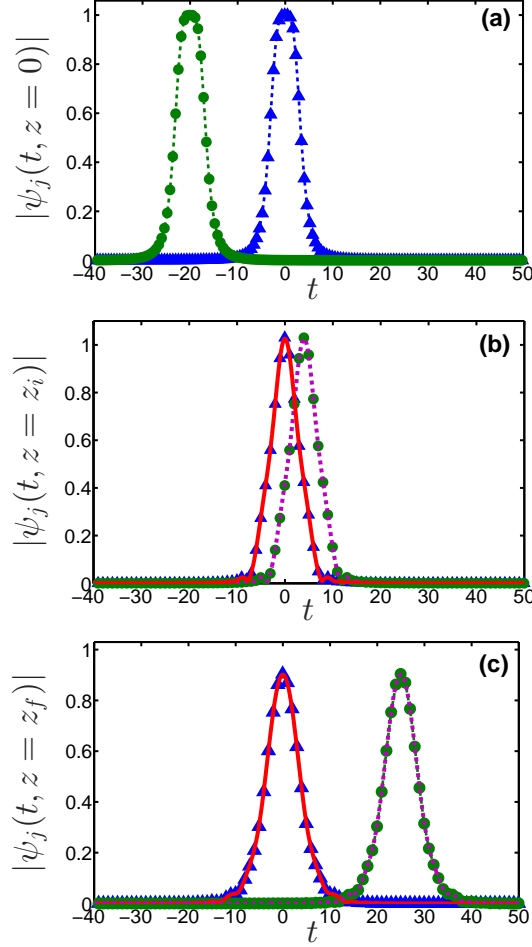


FIG. 3: (Color online) The pulse shapes  $|\psi_j(t, z)|$  at  $z = 0$  (a),  $z = z_i = 1.571$  (b), and  $z = z_f = 3$  (c) in a fast collision between two generalized Cauchy-Lorentz pulses in a linear waveguide with weak linear and cubic loss. The first-order dispersion coefficient is  $d_1 = 15$ . The blue triangles and green circles represent the initial pulse shapes  $|\psi_j(t, 0)|$  with  $j = 1, 2$  in (a), and the perturbation theory's prediction for  $|\psi_j(t, z)|$  with  $j = 1, 2$  in (b) and (c). The solid red and dashed magenta curves in (b) and (c) correspond to  $|\psi_j(t, z)|$  with  $j = 1, 2$ , obtained by numerical solution of Eq. (1).

faster than exponential decrease with time for the perturbation theory to hold. Moreover, our results demonstrate that the universal behavior of the collision-induced amplitude shift is also observed in collisions between pulses with a relatively slow decay of the tails, such as power-law decay.

We now turn to consider fast collisions between square pulses. The initial pulse shapes  $|\psi_j(t, 0)|$ , and the pulse shapes  $|\psi_j(t, z)|$  obtained in the simulation with  $d_1 = 15$  at the

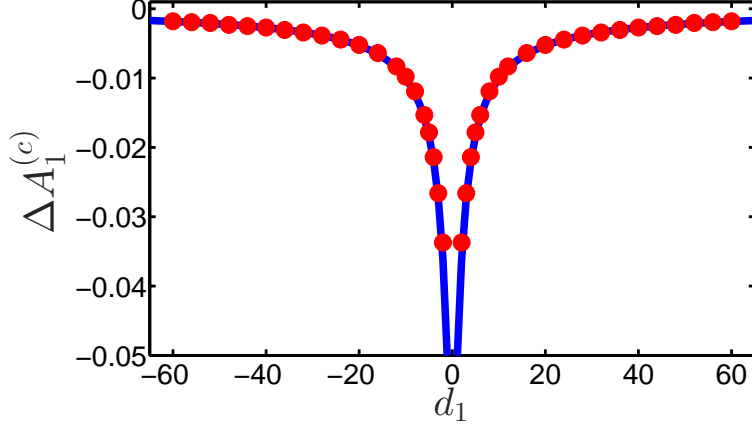


FIG. 4: (Color online) The collision-induced amplitude shift of pulse 1  $\Delta A_1^{(c)}$  vs the group velocity parameter  $d_1$  in a fast collision between two generalized Cauchy-Lorentz pulses in a linear waveguide with weak linear and cubic loss. The red circles represent the result obtained by numerical solution of Eq. (1). The solid blue curve represents the prediction of Eq. (17) with  $C_P = 3\pi/2^{7/4}$ .

intermediate distance  $z_i = 0.986 > z_c$  and at the final distance  $z_f = 4.5$  are shown in Fig. 5. The analytic prediction obtained with Eq. (5) is also shown. We observe that the pulses develop extended oscillatory tails and experience broadening due to the effects of second-order dispersion. The development of the extended tails occurs on a length scale in  $z$ , which is smaller than the collision length  $\Delta z_c$ . Despite of this fact, we observe very good agreement between the perturbation theory's prediction for the pulse shapes and the simulation's result at both  $z = z_i$  and  $z = z_f$ . The dependence of the collision-induced amplitude shift  $\Delta A_1^{(c)}$  on  $d_1$  obtained in the simulations is shown in Fig. 6 along with the analytic prediction of Eq. (17). The agreement between the analytic prediction and the results of the simulations is very good, despite of the development of extended pulse tails. More specifically, the relative error in the approximation of  $\Delta A_1^{(c)}$  is smaller than 3.8% for  $10 \leq |d_1| \leq 60$ , smaller than 7.2% for  $3 \leq |d_1| < 10$ , and is equal to 22.0% at  $|d_1| = 2$ . The good agreement between the analytic prediction and the results of the numerical simulations can be explained in the following manner. First, since  $\Delta z_c \ll z_D$ , most of the energy is contained in the main bodies of the pulses during the collision [see Fig. 5(b)]. Second, the total energy integrals  $\int_{-\infty}^{\infty} dt \tilde{\Psi}_{j0}^2(t, z)$ , which appear in the calculation of  $\Delta A_1^{(c)}$  [see Eqs. (14)-(16)], are conserved by the unperturbed linear propagation equation. As a result, the redistribution of the total energy of the pulses due to the development of extended tails does not have a significant effect

on the values of  $\Delta A_1^{(c)}$  measured in the simulations for  $|d_1| \geq 3$ , as long as the main bodies of the pulses are well-separated at  $z_f$ . Instead, contributions to the amplitude shift coming from interaction between the main body of one pulse and the tail of the other pulse and between the tails of both pulses partially compensate for the reduction in the contribution coming from direct interaction between the main bodies of the two pulses. Based on the results presented in Figs. 5 and 6 and on similar results obtained with other values of the physical parameters, we conclude that the universal behavior of the collision-induced amplitude shift can be observed even in collisions between pulses, which develop extended tails during the collision.

### III. FAST COLLISIONS IN SYSTEMS DESCRIBED BY COUPLED LINEAR DIFFUSION-ADVECTION MODELS

#### A. Evolution model and initial pulse shapes

We consider the dynamics of a fast collision between pulses of two substances, denoted by 1 and 2, that evolve in the presence of linear diffusion, weak linear and quadratic loss, and advection of material 2 with velocity  $v_d$  relative to material 1. The dynamics of the fast two-pulse collision is described by the following system of perturbed coupled linear diffusion-advection equations [19]:

$$\begin{aligned}\partial_t u_1 &= \partial_x^2 u_1 - \varepsilon_1 u_1 - \varepsilon_2 u_1^2 - 2\varepsilon_2 u_1 u_2, \\ \partial_t u_2 &= \partial_x^2 u_2 - v_d \partial_x u_2 - \varepsilon_1 u_2 - \varepsilon_2 u_2^2 - 2\varepsilon_2 u_1 u_2,\end{aligned}\tag{19}$$

where  $u_1$  and  $u_2$  are the concentrations of substance 1 and 2,  $t$  is time,  $x$  is a spatial coordinate, and the linear and quadratic loss coefficients  $\varepsilon_1$  and  $\varepsilon_2$  satisfy  $0 < \varepsilon_1 \ll 1$  and  $0 < \varepsilon_2 \ll 1$  [35]. The term  $-v_d \partial_x u_2$  in Eq. (19) describes advection, while the terms  $-\varepsilon_1 u_j$  describe the effects of linear loss. The terms  $-\varepsilon_2 u_j^2$  and  $-2\varepsilon_2 u_j u_k$  describe intra-substance and inter-substance effects due to quadratic loss, respectively. Note that in Eq. (19) we assume that the nonlinear loss is weak, and therefore, the effects of higher-order loss can be neglected. We point out that the effects of higher-order loss on the collision-induced amplitude shift can be calculated in a manner similar to the one described in Sec. IIIB (see also, Ref. [26], where a similar calculation was performed for collisions between Gaussian



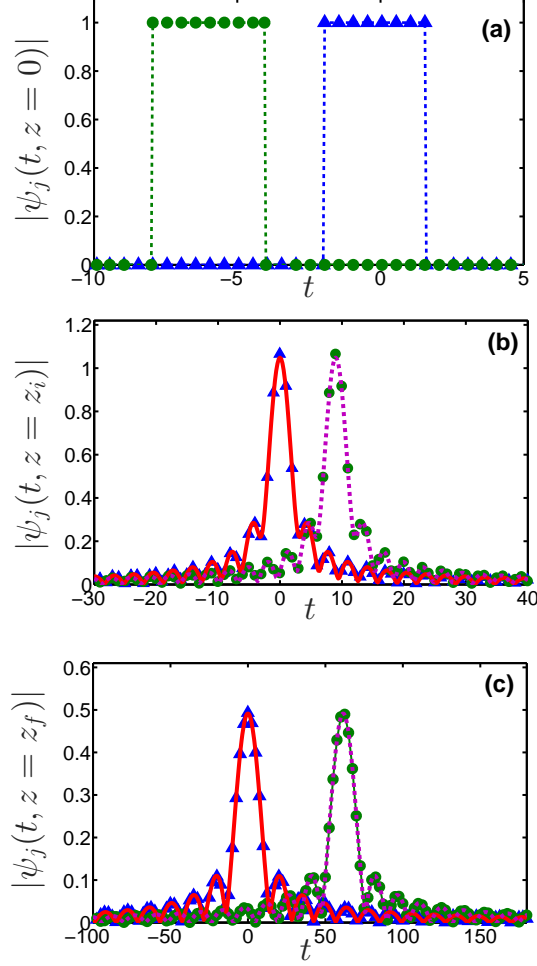


FIG. 5: (Color online) The pulse shapes  $|\psi_j(t, z)|$  at  $z = 0$  (a),  $z = z_i = 0.986$  (b), and  $z = z_f = 4.5$  (c) in a fast collision between two square pulses in a linear waveguide with weak linear and cubic loss. The first-order dispersion coefficient is  $d_1 = 15$ . The blue triangles and green circles represent the initial pulse shapes  $|\psi_j(t, 0)|$  with  $j = 1, 2$  in (a), and the perturbation theory's prediction for  $|\psi_j(t, z)|$  with  $j = 1, 2$  in (b) and (c). The solid red and dashed magenta curves in (b) and (c) correspond to  $|\psi_j(t, z)|$  with  $j = 1, 2$ , obtained by numerical solution of Eq. (1).

pulses in weakly perturbed linear optical waveguides).

We are interested in demonstrating universal behavior of the collision-induced amplitude shift. For this purpose, we consider fast collisions between pulses with generic initial shapes and with tails that decay sufficiently fast, such that the values of the integrals  $\int_{-\infty}^{\infty} dx u_j(x, 0)$  are finite. We assume that the pulses can be characterized by initial amplitudes  $A_j(0)$ , initial widths  $W_{j0}$ , and initial positions  $x_{j0}$ . Similar to Sec. II, we demonstrate the universal behavior of the collision-induced amplitude shift by considering the following three major

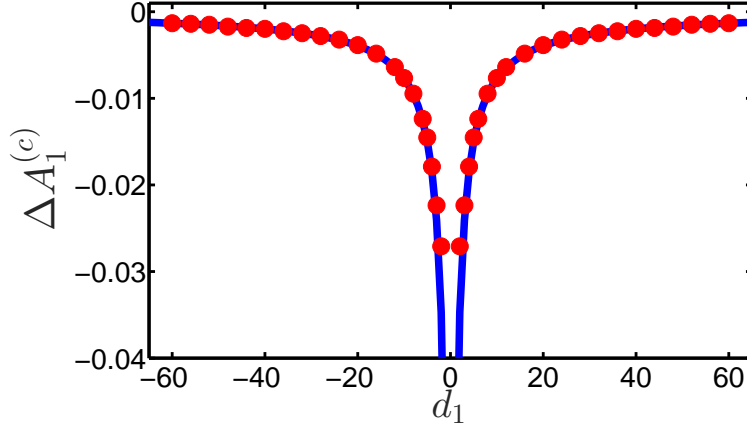


FIG. 6: (Color online) The collision-induced amplitude shift of pulse 1  $\Delta A_1^{(c)}$  vs the group velocity parameter  $d_1$  in a fast collision between two square pulses in a linear waveguide with weak linear and cubic loss. The red circles represent the result obtained by numerical simulations with Eq. (1). The solid blue curve corresponds to the prediction of Eq. (17) with  $C_P = 2$ .

types of pulses: (1) pulses with exponentially decreasing tails, (2) pulses with power-law decreasing tails, (3) pulses that are initially nonsmooth. For concreteness, we demonstrate the behavior of the amplitude shift using the following representative initial pulses: hyperbolic secant pulses in (1), generalized Cauchy-Lorentz pulses in (2), and square pulses in (3). The initial concentrations  $u_j(x, 0)$  for these pulses are given by

$$u_j(x, 0) = A_j(0) \operatorname{sech} [(x - x_{j0})/W_{j0}], \quad (20)$$

with  $j = 1, 2$  for hyperbolic secant pulses, by

$$u_j(x, 0) = \frac{A_j(0)}{1 + 2 [(x - x_{j0})/W_{j0}]^4}, \quad (21)$$

with  $j = 1, 2$  for generalized Cauchy-Lorentz pulses, and by

$$u_j(x, 0) = \begin{cases} A_j(0) & \text{for } |x - x_{j0}| \leq W_{j0}/2, \\ 0 & \text{for } |x - x_{j0}| > W_{j0}/2, \end{cases} \quad (22)$$

with  $j = 1, 2$  for square pulses. We point out that similar behavior of the collision-induced amplitude shift is observed for other choices of the initial pulse shapes.

## B. Calculation of the collision-induced amplitude shift

To obtain the expressions for the collision-induced amplitude shifts, we assume a complete fast two-pulse collision. The complete collision assumption means that the two pulses are well separated at  $t = 0$  and at the final time  $t = t_f$ . The assumption of a fast collision means that the collision time interval  $\Delta t_c = W_0/|v_d|$ , which is the time interval during which the two pulses overlap, is much shorter than the diffusion time  $t_D = W_0^2$ . Requiring  $\Delta t_c \ll t_D$ , we obtain  $W_0|v_d| \gg 1$ , as the condition for a fast collision.

We now demonstrate that the condition  $W_0|v_d| \gg 1$  for a fast collision can be realized in weakly perturbed physical systems described by linear diffusion-advection models. An important example for these systems is provided by binary gas mixtures. For concreteness, consider diffusion of  $O_2$  in  $N_2$  at  $293.15^\circ\text{K}$  and at a pressure of 1 atm. The diffusion coefficient is  $D = 0.202 \text{ cm}^2/\text{s}$  [36]. Thus, for an initial pulse width of 1 cm and for an advection velocity value of  $V_d = 3 \text{ cm/s}$ , we find that  $W_0|v_d| = 14.85$ . Similar results are obtained in other binary gas mixtures. For example, the diffusion coefficient of  $CO_2$  in  $N_2$  at  $293.15^\circ\text{K}$  and at a pressure of 1 atm is  $D = 0.160 \text{ cm}^2/\text{s}$  [36]. Using this value we find that for an initial pulse width of 1 cm and for  $V_d = 3 \text{ cm/s}$ ,  $W_0|v_d| = 18.75$ . Therefore, the condition  $W_0|v_d| \gg 1$  for a fast two-pulse collision is satisfied in both cases.

The perturbation technique for calculating the collision-induced amplitude shift is similar to the one derived in section II B for treating fast collisions between pulses of the linear propagation equation. Thus, we look for a solution of Eq. (19) in the form

$$u_j(x, t) = u_{j0}(x, t) + \phi_j(x, t), \quad (23)$$

where  $j = 1, 2$ ,  $u_{j0}$  are solutions of Eq. (19) without inter-pulse interaction, and  $\phi_j$  describe collision-induced effects. By definition,  $u_{10}$  and  $u_{20}$  satisfy the following two weakly perturbed linear diffusion equations

$$\partial_t u_{10} = \partial_x^2 u_{10} - \varepsilon_1 u_{10} - \varepsilon_2 u_{10}^2, \quad (24)$$

and

$$\partial_t u_{20} = \partial_x^2 u_{20} - v_d \partial_x u_{20} - \varepsilon_1 u_{20} - \varepsilon_2 u_{20}^2. \quad (25)$$

We substitute the ansatz (23) into Eq. (19) and use Eqs. (24) and (25) to obtain equations for  $\phi_1$  and  $\phi_2$ . We concentrate on the calculation of  $\phi_1$ , since the calculation of  $\phi_2$  is similar.

Taking into account only leading-order effects of the collision, we can neglect terms that contain products of  $\varepsilon_1$  or  $\varepsilon_2$  with  $\phi_1$  or  $\phi_2$ , such as  $-\varepsilon_1\phi_1$ ,  $-2\varepsilon_2u_{10}\phi_1$ ,  $-2\varepsilon_2u_{20}\phi_1$ ,  $-2\varepsilon_2u_{10}\phi_2$ , etc. We therefore obtain:

$$\partial_t\phi_1 = \partial_x^2\phi_1 - 2\varepsilon_2u_{10}u_{20}. \quad (26)$$

The term  $-2\varepsilon_2u_{10}u_{20}$  on the right hand side of Eq. (26) is of order  $\varepsilon_2$ . Additionally, the collision time interval  $\Delta t_c$  is of order  $1/|v_d|$  and therefore, the term  $\partial_t\phi_1$  is of order  $|v_d| \times O(\phi_1)$ . Equating the orders of  $\partial_t\phi_1$  and  $-2\varepsilon_2u_{10}u_{20}$ , we find that  $\phi_1$  is of order  $\varepsilon_2/|v_d|$ . As a result, the term  $\partial_x^2\phi_1$  is of order  $\varepsilon_2/|v_d|$  and can be neglected. Thus, the equation for the collision-induced change of pulse 1 in the leading order of the perturbative calculation is:

$$\partial_t\phi_1 = -2\varepsilon_2u_{10}u_{20}. \quad (27)$$

Equation (27) is similar to Eq. (10) in section II B and also to the equation obtained in Ref. [10] for a fast collision between two solitons of the NLS equation in the presence of weak cubic loss.

The net collision-induced amplitude shift of pulse 1 is calculated from the net collision-induced change in the concentration of pulse 1. We denote by  $t_c$  the collision time, which is the time at which the maxima of  $u_j(x, t)$  coincide. In a fast collision, the collision takes place in the small time interval  $[t_c - \Delta t_c, t_c + \Delta t_c]$  around  $t_c$ . Therefore, the net collision-induced change in the concentration of pulse 1  $\Delta\phi_1(x, t_c)$  can be estimated by:  $\Delta\phi_1(x, t_c) = \phi_1(x, t_c + \Delta t_c) - \phi_1(x, t_c - \Delta t_c)$ . To calculate  $\Delta\phi_1(x, t_c)$ , we introduce the approximation  $u_{j0}(x, t) = A_j(t)\tilde{u}_{j0}(x, t)$ , where  $\tilde{u}_{j0}(x, t)$  is the solution of the unperturbed linear diffusion equation with unit amplitude. Substituting the approximate expressions for  $u_{j0}$  into Eq. (27) and integrating with respect to time over the interval  $[t_c - \Delta t_c, t_c + \Delta t_c]$ , we obtain:

$$\Delta\phi_1(x, t_c) = -2\varepsilon_2 \int_{t_c - \Delta t_c}^{t_c + \Delta t_c} dt' A_1(t') A_2(t') \tilde{u}_{10}(x, t') \tilde{u}_{20}(x, t'). \quad (28)$$

The only function on the right hand side of Eq. (28) that contains fast variations in  $t$ , which are of order 1, is  $\tilde{u}_{20}$ . Therefore, we can approximate  $A_1(t)$ ,  $A_2(t)$ , and  $\tilde{u}_{10}(x, t)$  by  $A_1(t_c^-)$ ,  $A_2(t_c^-)$ , and  $\tilde{u}_{10}(x, t_c)$ . Additionally, we can take into account only the fast dependence of  $\tilde{u}_{20}$  on  $t$ , i.e., the  $t$  dependence that is contained in the factors  $y = x - x_{20} - v_d t$ . Denoting this

approximation of  $\tilde{u}_{20}(x, t)$  by  $\bar{u}_{20}(y, t_c)$  and implementing the approximations, we obtain:

$$\Delta\phi_1(x, t_c) = -2\varepsilon_2 A_1(t_c^-) A_2(t_c^-) \tilde{u}_{10}(x, t_c) \times \int_{t_c - \Delta t_c}^{t_c + \Delta t_c} dt' \bar{u}_{20}(x - x_{20} - v_d t', t_c). \quad (29)$$

Since the integrand on the right hand side of Eq. (29) is sharply peaked at a small interval about  $t_c$ , we can extend the integral's limits to  $-\infty$  and  $\infty$ . In addition, we change the integration variable from  $t'$  to  $y = x - x_{20} - v_d t'$  and obtain

$$\Delta\phi_1(x, t_c) = -\frac{2\varepsilon_2 A_1(t_c^-) A_2(t_c^-)}{|v_d|} \tilde{u}_{10}(x, t_c) \int_{-\infty}^{\infty} dy \bar{u}_{20}(y, t_c). \quad (30)$$

In Appendix A, we show that the net collision-induced amplitude shift of pulse 1  $\Delta A_1^{(c)}$  is related to  $\Delta\phi_1(x, t_c)$  by:

$$\Delta A_1^{(c)} = \left[ \int_{-\infty}^{\infty} dx \tilde{u}_{10}(x, t_c) \right]^{-1} \int_{-\infty}^{\infty} dx \Delta\phi_1(x, t_c). \quad (31)$$

Substituting Eq. (30) into Eq. (31), we arrive at the following expression for the total collision-induced amplitude shift of pulse 1:

$$\Delta A_1^{(c)} = -\frac{2\varepsilon_2 A_1(t_c^-) A_2(t_c^-)}{|v_d|} \int_{-\infty}^{\infty} dy \bar{u}_{20}(y, t_c). \quad (32)$$

We note that

$$\int_{-\infty}^{\infty} dy \bar{u}_{20}(y, t_c) = \int_{-\infty}^{\infty} dx \tilde{u}_{20}(x, t_c).$$

In addition, since  $\int_{-\infty}^{\infty} dx \tilde{u}_{20}(x, t)$  is a conserved quantity of the unperturbed linear diffusion equation, the following relations hold

$$\int_{-\infty}^{\infty} dx \tilde{u}_{20}(x, t_c) = \int_{-\infty}^{\infty} dx \tilde{u}_{20}(x, 0) = \text{const.}$$

Therefore, we can replace the integral on the right hand side of Eq. (32) by  $\int_{-\infty}^{\infty} dx \tilde{u}_{20}(x, 0)$  and obtain

$$\Delta A_1^{(c)} = -\frac{2\varepsilon_2 A_1(t_c^-) A_2(t_c^-)}{|v_d|} \int_{-\infty}^{\infty} dx \tilde{u}_{20}(x, 0). \quad (33)$$

We observe that the amplitude shift  $\Delta A_1^{(c)}$  depends only on the values of  $A_1(t_c^-)$ ,  $A_2(t_c^-)$ ,  $|v_d|$ , and on the initial total mass of pulse 2,  $\int_{-\infty}^{\infty} dx \tilde{u}_{20}(x, 0)$ . Since the expression for  $\Delta A_1^{(c)}$

is independent of the exact details of the initial pulse shapes, we say that this expression is universal. Equation (33) is expected to hold for generic pulse shapes  $u_{j0}(x, t)$  with tails that decay sufficiently fast, such that the approximations leading from Eq. (28) to Eq. (30) are valid. In Sec. III C, we show by numerical simulations with the coupled diffusion-advection model (19) that Eq. (33) is valid even for pulses with power-law decreasing tails, such as generalized Cauchy-Lorentz pulses, and for pulses that are initially nonsmooth, such as square pulses.

Using Eq. (33), we can obtain explicit expressions for the amplitude shifts in fast collisions between hyperbolic secant pulses, generalized Cauchy-Lorentz pulses, and square pulses, whose initial shapes are given by Eqs. (20), (21), and (22), respectively. We find that in all three cases,  $\Delta A_1^{(c)}$  is given by:

$$\Delta A_1^{(c)} = -C_D \varepsilon_2 W_{20} A_1(t_c^-) A_2(t_c^-) / |v_d|, \quad (34)$$

where the value of the constant  $C_D$  depends on the initial total mass of pulse 2. In addition, we find that  $C_D = 2\pi$  for a collision between hyperbolic secant pulses,  $C_D = 2^{1/4}\pi$  for a collision between generalized Cauchy-Lorentz pulses, and  $C_D = 2$  for a collision between square pulses. We point out that Eqs. (33) and (34) are similar to Eqs. (16) and (17) for the amplitude shift in a fast collision between two pulses of the linear propagation model in the presence of weak cubic loss. Equation (34) is also similar to Eq. (18) for the amplitude shift in a fast collision between two solitons of the NLS equation in the presence of weak cubic loss.

### C. Numerical simulations for different pulse shapes

To validate the predictions for universal behavior of the amplitude shift in fast two-pulse collisions, we carry out numerical simulations with Eq. (19). The equation is numerically solved by the split-step method with periodic boundary conditions [37]. For concreteness and without loss of generality, we present here the results of simulations with parameter values  $\varepsilon_1 = 0.01$  and  $\varepsilon_2 = 0.01$ . Since we are interested in fast collisions, the values of  $v_d$  are varied in the intervals  $-60 \leq v_d \leq -2$  and  $2 \leq v_d \leq 60$ . The universal behavior of the collision-induced amplitude shift is demonstrated by carrying out numerical simulations with the three typical initial pulse shapes given by Eqs. (20)-(22), i.e., with hyperbolic

secant pulses, generalized Cauchy-Lorentz pulses, and square pulses. The values of the initial amplitudes, initial widths, and initial position of pulse 1 are chosen as  $A_j(0) = 1$ ,  $W_{j0} = 4$ , and  $x_{10} = 0$ . The initial position of pulse 2  $x_{20}$  and the final time  $t_f$  are chosen, such that the pulses are well separated at  $t = 0$  and at  $t = t_f$ . More specifically, we choose  $x_{20} = \pm 25$  and  $t_f = 4$  for hyperbolic secant pulses,  $x_{20} = \pm 25$  and  $t_f = 3.5$  for generalized Cauchy-Lorentz pulses, and  $x_{20} = \pm 6$  and  $t_f = 1.5$  for square pulses. We point out that results similar to the ones presented below are obtained in numerical simulations with other physical parameter values. For each pulse shape type, we present the dependence of  $\Delta A_1^{(c)}$  on  $v_d$  obtained in the simulations along with the perturbation theory's prediction of Eq. (34). We also discuss the behavior of the relative error in the approximation of  $\Delta A_1^{(c)}$ . The procedures for calculating the values of  $\Delta A_1^{(c)}$  from Eq. (34) and from the results of the numerical simulations are similar to the ones described in Appendix B.

We first discuss the results of the numerical simulations for fast collisions between hyperbolic secant pulses. Figure 7 shows the pulse shapes  $u_j(x, t)$  obtained in the simulation with  $v_d = 15$  at  $t = 0$ , at the intermediate time  $t_i = 2 > t_c$ , and at the final time  $t_f = 4$  [38]. The analytic prediction for  $u_j(x, t)$ , obtained with Eq. (23), is also shown. We observe that the pulses experience broadening due to diffusion. Despite of the broadening, the agreement between the numerical result and the analytic prediction is very good at both  $t = t_i$  and  $t = t_f$ . Figure 8 shows the dependence of  $\Delta A_1^{(c)}$  on  $v_d$  obtained by the simulations along with the analytic prediction of Eq. (34). The agreement between the analytic prediction and the simulations results is very good. In particular, the relative error in the approximation of  $\Delta A_1^{(c)}$  is smaller than 4.1% for  $10 \leq |v_d| \leq 60$  and smaller than 13.3% for  $2 \leq |v_d| < 10$ . Similar behavior was observed in Ref. [19] for collisions between Gaussian pulses. Thus, our findings in the current paper and in Ref. [19] demonstrate the universal behavior of the amplitude shift in fast collisions between pulses, whose tails exhibit exponential or faster than exponential decrease with increasing distance from the pulse maximum.

Next, we present the results of numerical simulations for fast collisions between generalized Cauchy-Lorentz pulses. Figure 9 shows the pulse shapes  $u_j(x, t)$  obtained in the simulation with  $v_d = 15$  at  $t = 0$ ,  $t_i = 1.929 > t_c$ , and  $t_f = 3.5$ . Also shown is the analytic prediction for  $u_j(x, t)$ , which is obtained with Eq. (23). The agreement between the numerical result and the analytic prediction is very good at both  $t = t_i$  and  $t = t_f$  despite of the diffusion-induced broadening experienced by the pulses. Additionally, we do not observe any

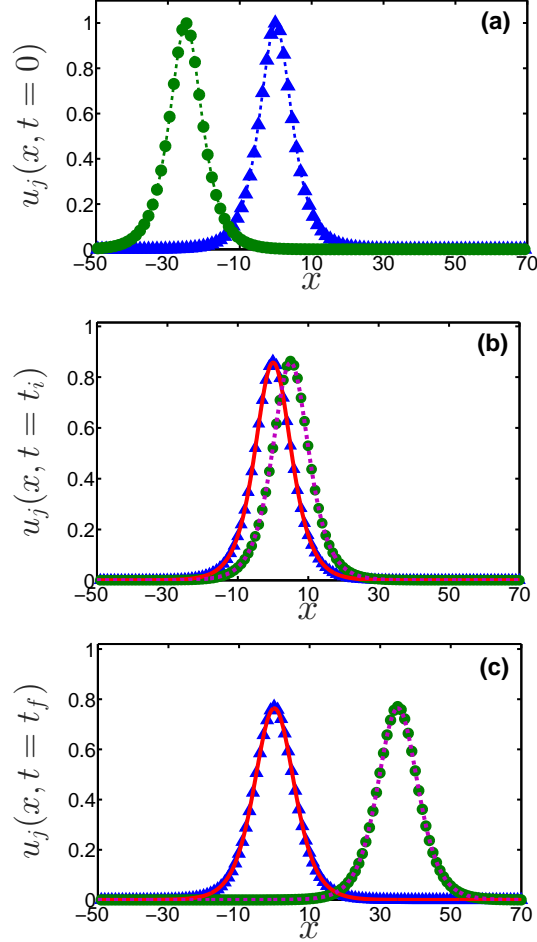


FIG. 7: (Color online) The pulse shapes  $u_j(x, t)$  at  $t = 0$  (a),  $t = t_i = 2$  (b), and  $t = t_f = 4$  (c) in a fast collision between two hyperbolic secant pulses in a system described by the coupled diffusion-advection model (19). The advection velocity is  $v_d = 15$ . The blue triangles and green circles represent the initial pulse shapes  $u_j(x, 0)$  with  $j = 1, 2$  in (a), and the perturbation theory's prediction for  $u_j(x, t)$  with  $j = 1, 2$  in (b) and (c). The solid red and dashed magenta curves in (b) and (c) correspond to  $u_j(x, t)$  with  $j = 1, 2$ , obtained by numerical solution of Eq. (19).

noticeable oscillatory features in the pulse tails, such as the ones seen in Figs. 3(b) and 3(c) for collisions between generalized Cauchy-Lorentz pulses in linear optical waveguides. The dependence of  $\Delta A_1^{(c)}$  on  $v_d$  obtained in the simulations is shown in Fig. 10 together with the analytic prediction of Eq. (34). We observe very good agreement between the results of the simulations and the analytic prediction. Indeed, the relative error in the approximation of  $\Delta A_1^{(c)}$  is less than 3.3% for  $10 \leq |v_d| \leq 60$  and less than 8.9% for  $2 \leq |v_d| < 10$ . Similar results are obtained for other values of the physical parameters and for other pulse shapes



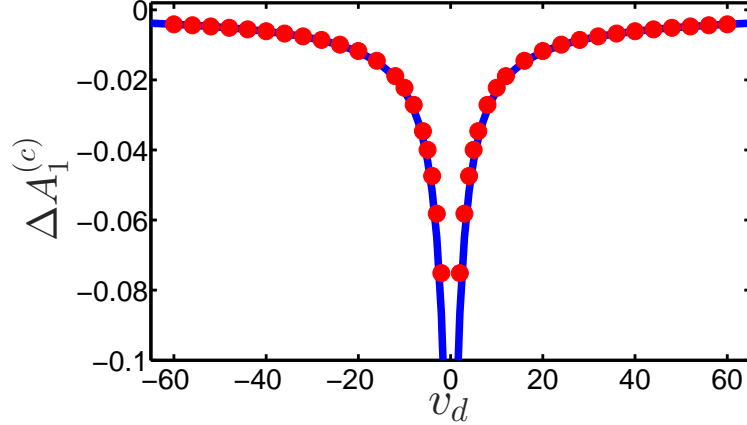


FIG. 8: (Color online) The collision-induced amplitude shift of pulse 1  $\Delta A_1^{(c)}$  vs advection velocity  $v_d$  in a fast collision between two hyperbolic secant pulses in a system described by the coupled diffusion-advection model (19). The red circles represent the result obtained by numerical solution of Eq. (19). The solid blue curve corresponds to the prediction of Eq. (34) with  $C_D = 2\pi$ .

with power-law decreasing tails. We therefore conclude that the universal behavior of the collision-induced amplitude shift is also observed in fast collisions between pulses, whose tails exhibit relatively slow (power-law) decrease with increasing distance from the pulse maximum.

Finally, we describe the results of the simulations for fast collisions between square pulses. The initial pulse shapes  $u_j(x, 0)$ , and the pulse shapes  $u_j(x, t)$  obtained in the simulation with  $v_d = 15$  at  $t = 0$ ,  $t_i = 0.557 > t_c$ , and  $t_f = 1.5$  is shown in Fig. 11. The analytic prediction, obtained with Eq. (23), is also shown. It is seen that the pulses undergo significant broadening due to the effects of diffusion. However, in contrast with the situation in linear optical waveguides, the pulses do not develop any observable oscillatory tails. Despite of the broadening, the agreement between the numerical result and the analytic prediction for the pulse shapes is very good. Figure 12 shows the dependence of  $\Delta A_1^{(c)}$  on  $v_d$  obtained by the simulations together with the analytic prediction of Eq. (34). We observe very good agreement between the analytic prediction and the simulations results. More specifically, the relative error in the approximation of  $\Delta A_1^{(c)}$  is smaller than 4.3% for  $10 \leq |v_d| \leq 60$  and smaller than 5.3% for  $2 \leq |v_d| < 10$ . Similar results are obtained with other values of the physical parameters. We therefore conclude that the universal behavior of the collision-induced amplitude shift can be observed even in collisions between pulses

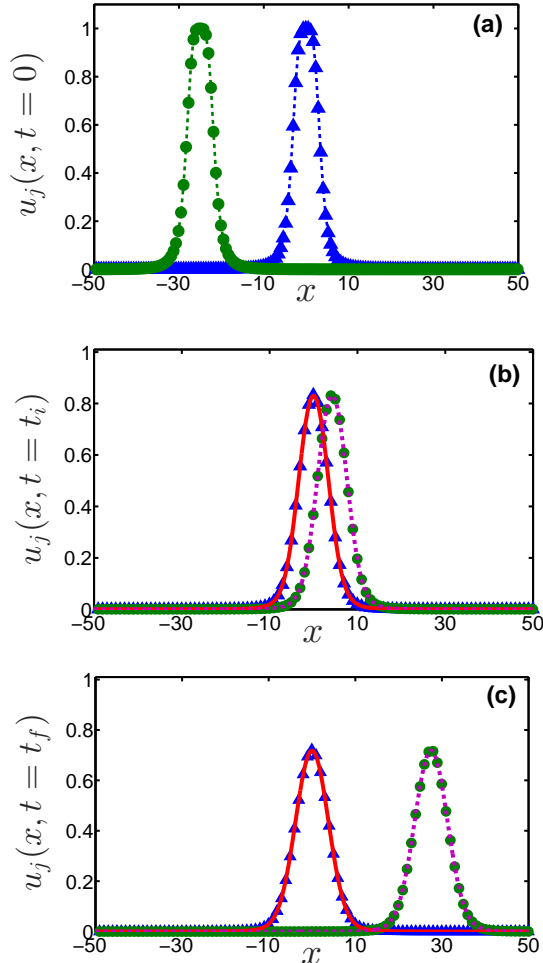


FIG. 9: (Color online) The pulse shapes  $u_j(x, t)$  at  $t = 0$  (a),  $t = t_i = 1.929$  (b), and  $t = t_f = 3.5$  (c) in a fast collision between two generalized Cauchy-Lorentz pulses in a system described by the coupled diffusion-advection model (19). The advection velocity is  $v_d = 15$ . The blue triangles and green circles represent the initial pulse shapes  $u_j(x, 0)$  with  $j = 1, 2$  in (a), and the perturbation theory's prediction for  $u_j(x, t)$  with  $j = 1, 2$  in (b) and (c). The solid red and dashed magenta curves in (b) and (c) correspond to  $u_j(x, t)$  with  $j = 1, 2$ , obtained by numerical solution of Eq. (19).

with nonsmooth initial shapes.

#### IV. CONCLUSIONS

We demonstrated that the amplitude shifts in fast two-pulse collisions in linear physical systems, weakly perturbed by nonlinear dissipation, exhibit universal soliton-like behavior.

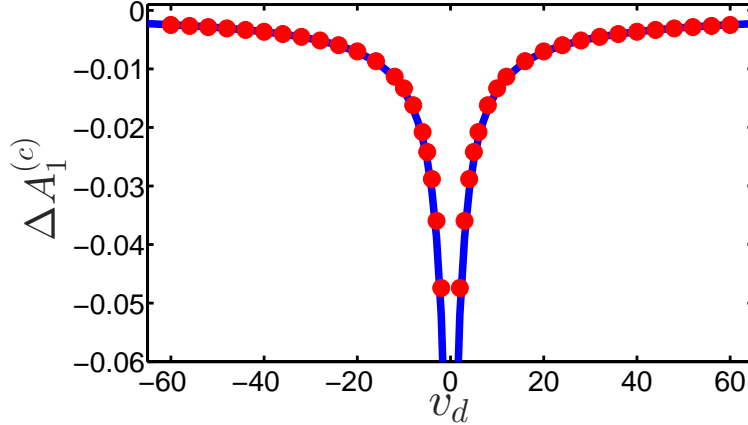


FIG. 10: (Color online) The collision-induced amplitude shift of pulse 1  $\Delta A_1^{(c)}$  vs advection velocity  $v_d$  in a fast collision between two generalized Cauchy-Lorentz pulses in a system described by the coupled diffusion-advection model (19). The red circles represent the result obtained by numerical solution of Eq. (19). The solid blue curve corresponds to the prediction of Eq. (34) with  $C_D = 2^{1/4}\pi$ .

The behavior was demonstrated for linear optical waveguides with weak cubic loss and for systems described by linear diffusion-advection models with weak quadratic loss. We showed that in both cases, the expressions for the collision-induced amplitude shifts due to the nonlinear loss have the same form as the expression for the amplitude shift in a fast collision between two solitons of the cubic NLS equation in the presence of weak cubic loss. Furthermore, we showed that the expressions for the amplitude shifts are universal in the sense that they are independent of the exact details of the initial pulse shapes. The universal soliton-like behavior of the expressions for the collision-induced amplitude shifts was explained by noting that changes in pulse shapes occurring during the collision due to the effects of dispersion or diffusion can be neglected for fast collisions, and by noting the conservation of the total energies (or total masses) of the pulses by the unperturbed linear evolution models. We demonstrated the universal behavior of the collision-induced amplitude shifts by performing numerical simulations with the two perturbed coupled linear evolution models with three different initial conditions corresponding to pulses with exponentially decreasing tails, pulses with power-law decreasing tails, and pulses that are initially nonsmooth. In all six cases we found very good agreement between the analytic predictions for the amplitude shifts and the results of the numerical simulations. Surprisingly, the analytic predictions held even

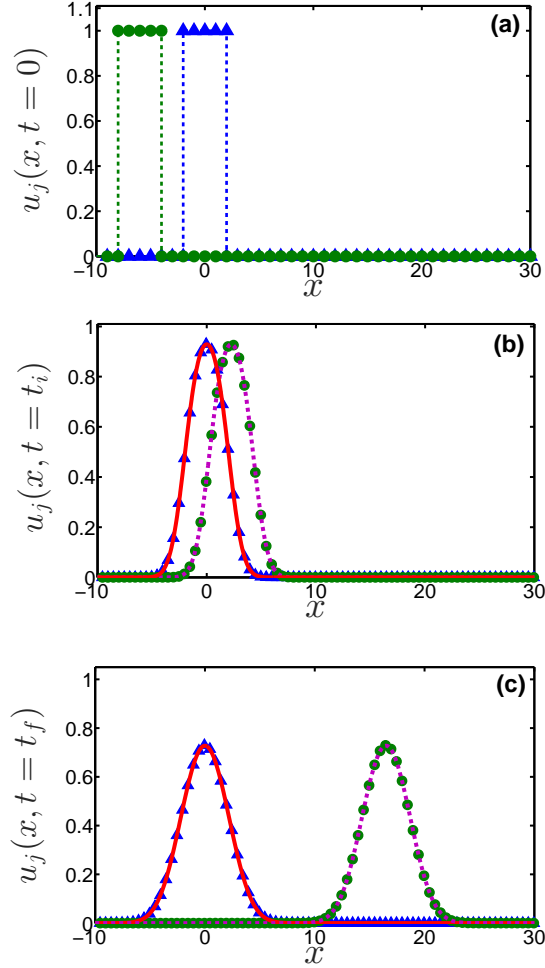


FIG. 11: (Color online) The pulse shapes  $u_j(x, t)$  at  $t = 0$  (a),  $t = t_i = 0.557$  (b), and  $t = t_f = 1.5$  (c) in a fast collision between two square pulses in a system described by the coupled diffusion-advection model (19). The advection velocity is  $v_d = 15$ . The blue triangles and green circles represent the initial pulse shapes  $u_j(x, 0)$  with  $j = 1, 2$  in (a), and the perturbation theory's prediction for  $u_j(x, t)$  with  $j = 1, 2$  in (b) and (c). The solid red and dashed magenta curves in (b) and (c) correspond to  $u_j(x, t)$  with  $j = 1, 2$ , obtained by numerical solution of Eq. (19).

for collisions between pulses with initially nonsmooth shapes in linear optical waveguides despite of the fast generation of significant pulse tails. The good agreement between the analytic and numerical results in the latter case was explained by noting that during fast collisions most of the pulse energies are still contained in the main bodies of the pulses, and by noting the conservation of the total energies of the two pulses by the unperturbed linear propagation model.

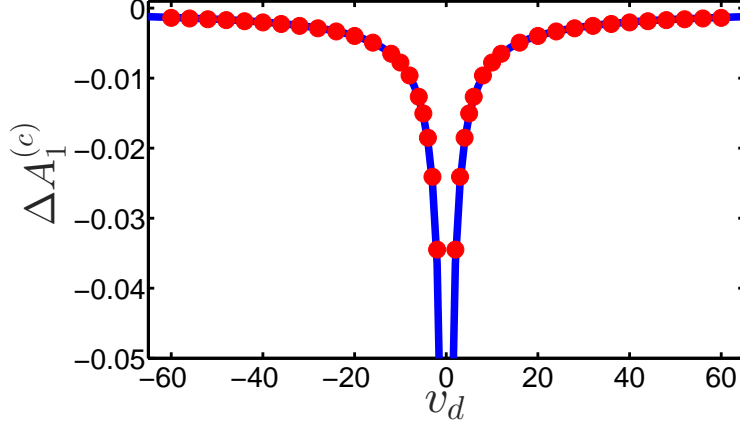


FIG. 12: (Color online) The collision-induced amplitude shift of pulse 1  $\Delta A_1^{(c)}$  vs advection velocity  $v_d$  in a fast collision between two square pulses in a system described by the coupled diffusion-advection model (19). The red circles represent the result obtained by numerical solution of Eq. (19). The solid blue curve corresponds to the prediction of Eq. (34) with  $C_D = 2$ .

### Acknowledgments

Q.M.N. and T.T.H. are supported by the Vietnam National Foundation for Science and Technology Development (NAFOSTED) under Grant No. 101.99-2015.29.

### Appendix A: Calculation of $\Delta A_1^{(c)}$ from $\Delta \Phi_1(t, z_c)$ and $\Delta \phi_1(x, t_c)$

In this Appendix, we derive relations (14) and (31) between the net collision-induced amplitude shift  $\Delta A_1^{(c)}$  and the net collision-induced changes in the envelope of the electric field and in material concentration  $\Delta \Phi_1(t, z_c)$  and  $\Delta \phi_1(x, t_c)$ . These relations were used to obtain Eq. (15) and Eq. (32) for  $\Delta A_1^{(c)}$  from Eqs. (13) and (30), respectively.

We first consider the linear waveguide system with weak linear and cubic loss, described by Eq. (1). To obtain the relation between  $\Delta A_1^{(c)}$  and  $\Delta \Phi_1(t, z_c)$ , we recall that the amplitude dynamics of a single pulse propagating in the presence of linear or nonlinear loss can be determined by an equation of the form  $\partial_z \int_{-\infty}^{\infty} dt |\psi_1(t, z)|^2 = \dots$ , where the right hand side of the equation is determined by the character of the loss perturbation [see for example Eq. (B1) in Appendix B]. A fast collision that takes place at a distance  $z = z_c$  leads to a jump in the value of  $\int_{-\infty}^{\infty} dt |\psi_1(t, z)|^2$  at  $z = z_c$ . Therefore, in this case, the term  $\partial_z \int_{-\infty}^{\infty} dt |\psi_1(t, z)|^2$  in the equation determining the dynamics of the amplitude should be replaced by the following

quantity:

$$\Delta_P = \int_{-\infty}^{\infty} dt |\psi_1(t, z_c^+)|^2 - \int_{-\infty}^{\infty} dt |\psi_1(t, z_c^-)|^2. \quad (\text{A1})$$

The relation between  $\Delta A_1^{(c)}$  and  $\Delta\Phi_1(t, z_c)$  is obtained by finding two expressions for  $\Delta_P$ , one involving  $\Delta A_1^{(c)}$  and the other involving  $\Delta\Phi_1(t, z_c)$ , and by equating the two expressions.

We note that by definition of  $\psi_{10}$  and  $\tilde{\Psi}_{10}$ ,  $\psi_1(t, z_c^-) \simeq \psi_{10}(t, z_c^-) \simeq A_1(z_c^-)\tilde{\Psi}_{10}(t, z_c) \exp[i\chi_{10}(t, z_c)]$ . Therefore, we can write

$$\int_{-\infty}^{\infty} dt |\psi_1(t, z_c^-)|^2 = C_1 A_1^2(z_c^-), \quad (\text{A2})$$

where  $C_1 = \int_{-\infty}^{\infty} dt \tilde{\Psi}_{10}^2(t, z_c)$  is a constant [39]. We also note that in the case of a fast collision, we can express  $\Delta\phi_1(t, z_c)$  as:  $\Delta\phi_1(t, z_c) \simeq \phi_1(t, z_c^+) - \phi_1(t, z_c^-) \simeq \phi_1(t, z_c^+)$ . Using this relation along with Eq. (5) and the definition of  $\psi_{10}$ , we obtain:

$$\psi_1(t, z_c^+) = \psi_{10}(t, z_c^-) + \Delta\phi_1(t, z_c). \quad (\text{A3})$$

Employing Eq. (A3) together with the definitions of  $\tilde{\Psi}_{10}$  and  $\Delta\Phi_1$ , we obtain:

$$\int_{-\infty}^{\infty} dt |\psi_1(t, z_c^+)|^2 = \int_{-\infty}^{\infty} dt \left[ A_1(z_c^-)\tilde{\Psi}_{10}(t, z_c) + \Delta\Phi_1(t, z_c) \right]^2 \quad (\text{A4})$$

Expanding the integrand on the right hand side of Eq. (A4), while keeping only the first two leading terms, we arrive at:

$$\begin{aligned} \int_{-\infty}^{\infty} dt |\psi_1(t, z_c^+)|^2 &\simeq C_1 A_1^2(z_c^-) \\ &+ 2A_1(z_c^-) \int_{-\infty}^{\infty} dt \tilde{\Psi}_{10}(t, z_c) \Delta\Phi_1(t, z_c). \end{aligned} \quad (\text{A5})$$

Substituting Eqs. (A2) and (A5) into Eq. (A1), we obtain the first expression for  $\Delta_P$ :

$$\Delta_P = 2A_1(z_c^-) \int_{-\infty}^{\infty} dt \tilde{\Psi}_{10}(t, z_c) \Delta\Phi_1(t, z_c). \quad (\text{A6})$$

On the other hand, we can express  $\int_{-\infty}^{\infty} dt |\psi_1(t, z_c^+)|^2$  in terms of  $\Delta A_1^{(c)}$  in the following manner:

$$\begin{aligned} \int_{-\infty}^{\infty} dt |\psi_1(t, z_c^+)|^2 &= \left( A_1(z_c^-) + \Delta A_1^{(c)} \right)^2 \int_{-\infty}^{\infty} dt \tilde{\Psi}_{10}^2(t, z_c) \\ &\simeq C_1 A_1^2(z_c^-) + 2C_1 A_1(z_c^-) \Delta A_1^{(c)}. \end{aligned} \quad (\text{A7})$$

Substituting Eqs. (A2) and (A7) into Eq. (A1), we find the second expression for  $\Delta_P$ :

$$\Delta_P = 2C_1 A_1(z_c^-) \Delta A_1^{(c)}. \quad (\text{A8})$$

Equating the right hand sides of Eqs. (A6) and (A8), we obtain:

$$\Delta A_1^{(c)} = \frac{1}{C_1} \int_{-\infty}^{\infty} dt \tilde{\Psi}_{10}(t, z_c) \Delta \Phi_1(t, z_c), \quad (\text{A9})$$

which is Eq. (14).

We now treat systems described by the coupled linear diffusion-advection model (19). The dynamics of the amplitude of a single pulse propagating in the presence of linear or nonlinear loss can be determined by an equation of the form  $\partial_t \int_{-\infty}^{\infty} dx u_1(x, t) = \dots$ , where the right hand side of the equation is determined by the nature of the loss perturbation. A fast collision that takes place at time  $t = t_c$  leads to a jump in the value of  $\int_{-\infty}^{\infty} dx u_1(x, t)$  at  $t = t_c$ . Therefore, in the fast collision problem, the term  $\partial_t \int_{-\infty}^{\infty} dx u_1(x, t)$  in the equation that determines the dynamics of the pulse amplitude should be replaced by:

$$\Delta_D = \int_{-\infty}^{\infty} dx u_1(x, t_c^+) - \int_{-\infty}^{\infty} dx u_1(x, t_c^-). \quad (\text{A10})$$

We now find two expressions for  $\Delta_D$ , one that depends on  $\Delta A_1^{(c)}$  and the other that depends on  $\Delta \phi_1(x, t_c)$ . The relation between  $\Delta A_1^{(c)}$  and  $\Delta \phi_1(x, t_c)$  is obtained by equating the two expressions.

By the definitions of  $u_1$ ,  $u_{10}$ , and  $\tilde{u}_{10}$ ,  $u_1(x, t_c^-) \simeq u_{10}(x, t_c^-) \simeq A_1(t_c^-) \tilde{u}_{10}(x, t_c)$ . It follows that

$$\int_{-\infty}^{\infty} dx u_1(x, t_c^-) = C_2 A_1(t_c^-), \quad (\text{A11})$$

where  $C_2 = \int_{-\infty}^{\infty} dx \tilde{u}_{10}(x, t_c)$  is a constant [40]. In addition, in a fast collision, we can express  $\Delta \phi_1(x, t_c)$  as:  $\Delta \phi_1(x, t_c) \simeq \phi_1(x, t_c^+) - \phi_1(x, t_c^-) \simeq \phi_1(x, t_c^+)$ . Using this relation together with Eq. (23) and the definition of  $u_{10}$ , we obtain

$$u_1(x, t_c^+) = u_{10}(x, t_c^-) + \Delta \phi_1(x, t_c). \quad (\text{A12})$$

From Eq. (A12), it follows that

$$\int_{-\infty}^{\infty} dx u_1(x, t_c^+) = \int_{-\infty}^{\infty} dx [u_{10}(x, t_c^-) + \Delta \phi_1(x, t_c)]. \quad (\text{A13})$$

Using the definition of  $\tilde{u}_{10}$  in Eq. (A13), we arrive at

$$\int_{-\infty}^{\infty} dx u_1(x, t_c^+) = C_2 A_1(t_c^-) + \int_{-\infty}^{\infty} dx \Delta\phi_1(x, t_c). \quad (\text{A14})$$

Substituting Eqs. (A11) and (A14) into Eq. (A10), we obtain the first expression for  $\Delta_D$ :

$$\Delta_D = \int_{-\infty}^{\infty} dx \Delta\phi_1(x, t_c). \quad (\text{A15})$$

On the other hand, we can express  $\int_{-\infty}^{\infty} dx u_1(x, t_c^+)$  in terms of  $\Delta A_1^{(c)}$  in the following way:

$$\begin{aligned} \int_{-\infty}^{\infty} dx u_1(x, t_c^+) &= \left( A_1(t_c^-) + \Delta A_1^{(c)} \right) \int_{-\infty}^{\infty} dx \tilde{u}_{10}(x, t_c) \\ &= C_2 A_1(t_c^-) + C_2 \Delta A_1^{(c)}. \end{aligned} \quad (\text{A16})$$

Substituting Eqs. (A11) and (A16) into Eq. (A10), we obtain the second expression for  $\Delta_D$ :

$$\Delta_D = C_2 \Delta A_1^{(c)}. \quad (\text{A17})$$

Equating the right hand sides of Eqs. (A15) and (A17), we obtain:

$$\Delta A_1^{(c)} = \frac{1}{C_2} \int_{-\infty}^{\infty} dx \Delta\phi_1(x, t_c), \quad (\text{A18})$$

which is Eq. (31).

## Appendix B: Methods for calculating the values of $\Delta A_1^{(c)}$ from the analytic predictions and from numerical simulations

In this appendix, we describe the methods used for obtaining the values of the collision-induced amplitude shift  $\Delta A_1^{(c)}$  from the analytic predictions and from results of numerical simulations. We demonstrate the implementation of these methods for a collision between pulses with generic shapes in a linear optical waveguide with weak linear and cubic loss. The implementation of the methods for collisions in physical systems described by linear diffusion-advection models is similar.

The analytic prediction for  $\Delta A_1^{(c)}$  is obtained by employing Eq. (16). The values of  $A_j(z_c^-)$  appearing in this equation are calculated by solving approximate equations for the dynamics of the  $A_j(z)$  for a single pulse, propagating in the presence of first and second-order dispersion, linear loss, and cubic loss. More specifically, single-pulse propagation of



pulse 1 is described by Eq. (6) and single-pulse propagation of pulse 2 is described by Eq. (7). Employing energy balance calculations for these two propagation models, we obtain

$$\partial_z \int_{-\infty}^{\infty} dt |\psi_{j0}|^2 = -2\epsilon_1 \int_{-\infty}^{\infty} dt |\psi_{j0}|^2 - 2\epsilon_3 \int_{-\infty}^{\infty} dt |\psi_{j0}|^4. \quad (\text{B1})$$

We express the approximate solutions of Eq. (6) and (7) as  $\psi_{j0}(t, z) = A_j(z)\tilde{\psi}_{j0}(t, z)$ , where  $\tilde{\psi}_{j0}(t, z) = \tilde{\Psi}_{j0}(t, z) \exp[i\chi_{j0}(t, z)]$  is the solution of the unperturbed linear propagation equation with initial amplitude  $A_j(0) = 1$ . Substituting the approximate expressions for  $\psi_{j0}(t, z)$  into Eq. (B1), we obtain:

$$\frac{d}{dz} [I_{2j}A_j^2] = -2\epsilon_1 I_{2j}A_j^2 - 2\epsilon_3 I_{4j}(z)A_j^4, \quad (\text{B2})$$

where  $I_{2j} = \int_{-\infty}^{\infty} dt \tilde{\Psi}_{j0}^2(t, z) = \int_{-\infty}^{\infty} dt \tilde{\Psi}_{j0}^2(t, 0) = \text{const}$  and  $I_{4j}(z) = \int_{-\infty}^{\infty} dt \tilde{\Psi}_{j0}^4(t, z)$ . Equation (B2) is a Bernoulli equation for  $A_j^2(z)$ . Its solution on the interval  $[0, z_c]$  yields the following expression for  $A_j(z_c^-)$ :

$$A_j(z_c^-) = \frac{A_j(0)e^{-\epsilon_1 z_c}}{\left[1 + 2\epsilon_3 \tilde{I}_{4j}(0, z_c)A_j^2(0)/I_{2j}\right]^{1/2}}, \quad (\text{B3})$$

where

$$\tilde{I}_{4j}(z_1, z_2) = \int_{z_1}^{z_2} dz I_{4j}(z)e^{-2\epsilon_1 z}. \quad (\text{B4})$$

We obtain the analytic prediction for  $\Delta A_1^{(c)}$  by calculating the values of  $A_j(z_c^-)$  with Eq. (B3) and by substituting these values into Eq. (16).

We obtain the value of  $\Delta A_1^{(c)}$  from the results of the numerical simulations by using the relation

$$\Delta A_1^{(c)} = A_1(z_c^+) - A_1(z_c^-), \quad (\text{B5})$$

where  $A_1(z_c^-)$  is calculated with Eq. (B3), and  $A_1(z_c^+)$  is determined from the simulations. More specifically, we solve Eq. (B2) with  $j = 1$  on the interval  $[z_c, z_f]$  and obtain

$$A_1(z_c^+) = \frac{A_1(z_f)e^{-\epsilon_1 z_c}}{\left[e^{-2\epsilon_1 z_f} - 2\epsilon_3 \tilde{I}_{41}(z_c, z_f)A_1^2(z_f)/I_{21}\right]^{1/2}}. \quad (\text{B6})$$

We then determine the value of  $A_1(z_c^+)$  by using Eq. (B6) with a value of  $A_1(z_f)$ , which is measured from the simulations.

---

[1] G.P. Agrawal, *Nonlinear Fiber Optics* (Academic, San Diego, CA, 2001).

- [2] L.F. Mollenauer and J.P. Gordon, *Solitons in Optical Fibers: Fundamentals and Applications* (Academic, San Diego, CA, 2006).
- [3] Y.S. Kivshar and B.A. Malomed, Rev. Mod. Phys. **61**, 763 (1989).
- [4] S. Novikov, S.V. Manakov, L.P. Pitaevskii, and V.E. Zakharov, *Theory of Solitons: The Inverse Scattering Method* (Plenum, New York, 1984).
- [5] A.C. Newell, *Solitons in Mathematics and Physics* (SIAM, Philadelphia, 1985).
- [6] W. Horton and Y.H. Ichikawa, *Chaos and Structure in Nonlinear Plasmas* (World Scientific, Singapore, 1996).
- [7] Fast soliton collisions are collisions for which the difference between the central frequencies (or group velocities) of the solitons is much larger than the soliton spectral width.
- [8] L.F. Mollenauer and P.V. Mamyshev, IEEE J. Quantum Electron. **34**, 2089 (1998).
- [9] Y. Chung and A. Peleg, Nonlinearity **18**, 1555 (2005).
- [10] A. Peleg, Q.M. Nguyen, and Y. Chung, Phys. Rev. A **82**, 053830 (2010).
- [11] S. Chi and S. Wen, Opt. Lett. **14**, 1216 (1989).
- [12] B.A. Malomed, Phys. Rev. A **44**, 1412 (1991).
- [13] S. Kumar, Opt. Lett. **23**, 1450 (1998).
- [14] A. Peleg, Opt. Lett. **29**, 1980 (2004).
- [15] Q.M. Nguyen and A. Peleg, J. Opt. Soc. Am. B **27**, 1985 (2010).
- [16] A. Peleg and Y. Chung, Phys. Rev. A **85**, 063828 (2012).
- [17] F. Forghieri, R.W. Tkach, and A.R. Chraplyvy, in *Optical Fiber Telecommunications III*, I.P. Kaminow and T.L. Koch, eds., (Academic, San Diego, CA, 1997), Chapter 8.
- [18] G.P. Agrawal, P.L. Baldeck, and R.R. Alfano, Phys. Rev. A **39**, 3406 (1989).
- [19] A. Peleg, Q.M. Nguyen, and T.T. Huynh, Eur. Phys. J. D **71**, 315 (2017).
- [20] Q. Lin, O.J. Painter, and G.P. Agrawal, Opt. Express **15**, 16604 (2007).
- [21] The dimensionless distance  $z$  in Eq. (1) is  $z = Z/(2L_D)$ , where  $Z$  is the dimensional distance,  $L_D = \tau_0^2/|\tilde{\beta}_2|$  is the dispersion length, and  $\tau_0$  is a reference pulse width. The dimensionless time is  $t = \tau/\tau_0$ , where  $\tau$  is time.  $\psi_j = E_j/\sqrt{P_0}$ , where  $E_j$  is the electric field of the  $j$ th pulse and  $P_0$  is peak power.  $d_1 = 2(\tilde{\beta}_{12} - \tilde{\beta}_{11})\tau_0/|\tilde{\beta}_2|$ , where  $\tilde{\beta}_{1j} = n_{gj}/c = 1/v_{gj}$ ,  $c$  is the speed of light, and  $n_{gj}$  and  $v_{gj}$  are the group refractive index and the group velocity for the  $j$ th pulse.  $\epsilon_1 = 2\tau_0^2\tilde{\rho}_1/|\tilde{\beta}_2|$  and  $\epsilon_3 = 2P_0\tau_0^2\tilde{\rho}_3/|\tilde{\beta}_2|$ , where  $\tilde{\rho}_1$  and  $\tilde{\rho}_3$  are the dimensional linear and cubic loss coefficients.

- [22] J.E. Ehrlich, X.L. Wu, I.-Y.S. Lee, Z.-Y. Hu, H. Röckel, S.R. Marder, and J.W. Perry, *Opt. Lett.* **22**, 1843 (1997).
- [23] T.K. Liang, L.R. Nunes, T. Sakamoto, K. Sasagawa, T. Kawanishi, M. Tsuchiya, G.R.A. Priem, D. Van Thourhout, P. Dumon, R. Baets, and H.K. Tsang, *Opt. Express* **13**, 7298 (2005).
- [24] R. Jones, H. Rong, A. Liu, A. Fang, M. Paniccia, D. Hak, and O. Cohen, *Opt. Express* **13**, 519 (2005).
- [25] A. Liu, H. Rong, M. Paniccia, O. Cohen and D. Hak, *Opt. Express* **12**, 4261 (2004).
- [26] Q.M. Nguyen, “Collision-induced amplitude dynamics of pulses in linear waveguides with the generic nonlinear loss”, arXiv:1808.02396, submitted.
- [27] L.F. Mollenauer, A. Grant, X. Liu, X. Wei, C. Xie, and I. Kang, *Opt. Lett.* **28**, 2043 (2003).
- [28] I.H. Malitson, *J. Opt. Soc. Am.* **55**, 1205 (1965).
- [29] C.Z. Tan, *J. Non-Cryst. Solids* **223**, 158 (1998).
- [30] D.E. Aspnes and A.A. Studna, *Phys. Rev. B* **27**, 985 (1983).
- [31] A. Peleg, M. Chertkov, and I. Gabitov, *Phys. Rev. E* **68**, 026605 (2003).
- [32] A. Peleg, M. Chertkov, and I. Gabitov, *J. Opt. Soc. Am. B* **21**, 18 (2004).
- [33] J. Yang, *Nonlinear Waves in Integrable and Nonintegrable Systems* (SIAM, Philadelphia, 2010).
- [34] The values of  $z_i$  are determined by the equation  $z_i = z_c + r(z_f - z_c)$ , where  $z_c = (y_{10} - y_{20})/d_1$ , and  $r = 1/7$ , as an example. Thus,  $z_i$  is an intermediate distance that is larger than  $z_c$ , at which the collision is not yet completed.
- [35] The dimensionless coordinate  $x$  in Eq. (19) is  $x = X/x_0$ , where  $X$  is the dimensional coordinate, and  $x_0$  is a reference pulse width. The dimensionless time is  $t = \tau/\tau_D$ , where  $\tau$  is time,  $\tau_D = x_0^2/D$ , and  $D$  is the diffusion coefficient.  $u_j = U_j/\rho_0$ , where  $U_j$  is the concentration of substance  $j$  and  $\rho_0$  is the peak concentration.  $v_d = x_0 V_d/D$ , where  $V_d$  is the dimensional advection velocity.  $\varepsilon_1 = x_0^2 \tilde{\varepsilon}_1/D$  and  $\varepsilon_2 = \rho_0 x_0^2 \tilde{\varepsilon}_2/D$ , where  $\tilde{\varepsilon}_1$  and  $\tilde{\varepsilon}_2$  are the dimensional linear and quadratic loss coefficients.
- [36] D.R. Lide, ed., *CRC Handbook of Chemistry and Physics* (CRC Press, Boca Raton, FL, 2004).
- [37] W.H. Hundsdorfer and J.G. Verwer, *Numerical Solution of Time Dependent Advection-Diffusion-Reaction Equations* (Springer, New York, 2003).
- [38] The values of  $t_i$  are determined by the equation  $t_i = t_c + r(t_f - t_c)$ , where  $t_c = (x_{10} - x_{20})/v_d$ ,

and  $r = 1/7$ , as an example. Thus,  $t_i$  is an intermediate time that is larger than  $t_c$ , at which the collision is not yet completed.

[39] Since the integral  $\int_{-\infty}^{\infty} dt \tilde{\Psi}_{10}^2(t, z)$  is conserved by the unperturbed linear propagation equation, we can write:  $C_1 = \int_{-\infty}^{\infty} dt \tilde{\Psi}_{10}^2(t, 0)$ .

[40] Since the integral  $\int_{-\infty}^{\infty} dx \tilde{u}_{10}(x, t)$  is conserved by the unperturbed linear diffusion equation, we can write:  $C_2 = \int_{-\infty}^{\infty} dx \tilde{u}_{10}(x, 0)$ .